NACA TM 1200

7865

TECH LIBRARY KAFB, NM
0144653

NATIONAL ADVISORY COMMITTEE FOR AERONAUTICS

TECHNICAL MEMORANDUM 1200

MEASUREMENT OF OIL-FILM PRESSURES IN JOURNAL BEARINGS UNDER CONSTANT AND VARIABLE LOADS

By A. Buske and W. Rolli

Translation of "Messung des Ölfilmdruckes in ruhend- und wechselnd belasteten Gleitlagern."
Jahrbuch 1937 der deutschen Luftfahrtforschung

Washington
November 1949

AFMDC
TECHNICAL LIBRARY
AFL 2811

TECH LIBRARY KAFB, NM

0144653

NATIONAL ADVISORY COMMITTEE FOR AERONAUTICS

TECHNICAL MEMORANDUM NO. 1200

MEASUREMENT OF OIL-FILM PRESSURES IN JOURNAL BEARINGS UNDER CONSTANT AND VARIABLE LOADS*

By A. Buske and W. Rolli

In a study of journal bearings, the measurement of the oil-film strength produces some significant information. A new instrument is described by means of which the pressure of the oil film in bearings (under constant or alternating load) can be measured and recorded. With this device, the pressure distribution in the lubricating film of a bearing bushing was measured (under different operating conditions on a journal bearing) in the pulsator-bearing-testing machine. These tests are described and discussed in the present report.

SUMMARY

The first part of the present report describes an instrument with which the oil pressure in the lubricating film of journal bearings under constant and alternating load can be measured and recorded in its time rate of change. Simplicity of design, smallness of size, high rate of response and point-like test stations make the instrument suitable for the present purposes. The instrumental accuracy was checked by an error calculation and by comparisons with the DVL glow discharge lamp indicator and the Zeiss-Ikon quartz indicator.

The second part deals with the actual measurements. The pressure in the oil film of an experimental bearing loaded in the DVL pulsator-bearing-testing machine was investigated as to its local distribution and its time rate of change under various operating conditions. The results, represented in diagrams, give a comprehensive view of the pressure distribution along, and transverse to, the direction of rotation. From the recorded diagrams the time-phase displacement of the maximum pressures at the several test points was determined and the shaft motion deduced. The oil film pressure measurements enable, further, the load capacity limit of the bearing at which the fluid friction changes to semifluid friction to be identified. In the continuation of the experiments the tests should include, aside from constructive influences of the bearing design, a more accurate investigation of the lubricating oil properties.

---

*"Messung des Ölfilmdruckes in ruhend- und wechselnd belasteten Gleitlagern." Jahrbuch 1937 der deutschen Luftfahrtforschung, pp. II 67 - II 78.

THE MEASURING EQUIPMENT

(a) Test Method

The majority of bearing investigations conducted so far deal with constant loads (references 1 to 5), while those made under alternating loads are usually limited to measurements of the oil flow between bearing and shaft and to temperature determinations (reference 6), and disregard the identification of the pressure variation in the oil film and the measurement of the shaft displacement.

The present task involved the design of a device with which the pressure in the oil film of bearings could be measured under constant and alternating loads.

Such a device must meet the following conditions:

(1) The oil film must not be disturbed at the point of measurement; hence, the bearing surface shall manifest no depression or elevation at that point. In addition, no oil must enter or leave at the point of measurement, as that would falsify the test data.

(2) The superficial extent of the point of measurement shall be held to a minimum, so that the film pressure is measured at one certain point only.

(3) The device must be small and easy to attach to the bushing so as to permit the use of several such devices on the experimental bearing for the study of the local pressure distribution in the film and insure their application in restricted space.

(4) The device must be suitable for dependable measurement of rapidly varying film pressure, of the maximum pressure under alternating load and for the recording of time-pressure curves The pickup must therefore have a high rate of response.

The problem was solved with a device which operates on the back pressure principle so successfully employed on the DVL glow discharge lamp (references 7 and 8).

The apparatus consists essentially of a small piston moving between two stops, one side of the piston being acted on by the oil film pressure, the other by the adjustable back pressure. If the pressure in the oil film predominates, the piston closes a contact which causes the glow-discharge lamp to light up. The burning periods of the lamp are photographically recorded as dashes in abscissa direction on paper revolving at shaft speed. The back pressure controls, at the same time, a rotating mirror which determines the position of these dashes in direction of the ordinate.

The method is suitable only for recording strictly periodic pressure variations; however, quite apart from its simplicity compared to other methods (such as electric indication with quartz or carbon plate column, mechanical indication by scratch record, for example), its essential advantage lies in its insusceptibility to temperature variations and minimum leakage losses since the back pressure (oil pressure) is equal to the film pressure at the instant of measurement. The limitation of the applicability to periodic processes is secondary for the present purposes.

(b) Description of the Instrument

1. Pickup.- The pickup is represented sectionalized in figure 1. It consists of the main body g threaded into the bearing shell so that the tubular piston guide and the frontal surface of the piston are flush with the bearing surface. The measuring piston k housed in body g has a diameter of 1 millimeter and weighs but 0.16 gram. Owing to these small dimensions of the piston the oil film pressure is actually determined at points. The cylindrical head of the piston, which is fitted with a support of contact metal and serves as stop for the piston stroke, is slightly backed off and milled so that the back pressure prevailing inside of the main body g admits only the actual 1-millimeter piston area. The tube r serves as fixed countercontact and for the supply of the back pressure produced by oil under pressure from a manometer-calibration pump. The tube r is electrically insulated by Pertinax plates and tube p from the main body which is grounded. The whole unit is held together by cap screw m. The piston can move back and forth for 0.02 to 0.1 millimeter, depending upon the setting of the insulating plates. Since the film pressure acts from the outside and the back pressure from the inside on the same piston area, the piston closes the contact as long as the film pressure is higher than the back pressure. If the back pressure is higher, the contact opens. At the moment of switching, the two pressures are equal up to a very small difference caused by piston friction and the subsequently discussed "acceleration error," so that, at the instant of actual measurement, no oil leaves or enters the bearing through the piston slot; hence, the oil film is not affected. The outside diameter of the entire pickup is only 8 millimeters, so that it is easily mounted in limited space. Figure 2 shows the pickup exploded, assembled, and installed in a bearing shell.

In preliminary tests with several pickups, the piston on which the film pressure acts was attached to a diaphragm on which the back pressure was to act, but such pickups exhibited considerable hysteresis, which was probably induced by the diaphragm restraint. Attempts with a partially cut-out diaphragm and with two very thin diaphragms were likewise unsatisfactory, so the diaphragm-controlled piston was finally abandoned in favor of the freely moving piston without restoring force.

2. The indicating mechanism.- A simple glow discharge lamp was used to indicate the oil-film pressure in bearings under constant load and to establish the extreme pressure of the oil film at the test point in bearings variable under alternating loads, the back pressure being raised by means of the hand pump (fig. 3) until the glow discharge lamp ceased to light up, and the pressure was read at that instant on the manometer.

The time-pressure diagrams were taken with the recording apparatus of the DVL indicator, the fundamental design of which is seen from figure 3. The light of the point-glow discharge lamp controlled by the pickup falls across a rotating mirror through a copying lens on photographic paper wound on a cylinder and synchronized with the process that is to be recorded. The rotating mirror is controlled by a tubular spring loaded by the back pressure and effectuates the focusing of the luminous point on the photographic paper in direction of the ordinates of the diagram.

For many tests, a small glow discharge lamp rotating with the alternating load frequency is also very suitable as indicating device. This glow discharge lamp describes a luminous arc for the eye of the observer, which becomes continuously shorter with increasing back pressure until finally only a very short light flash occurs. The lamp revolves in front of a graduated scale, thus affording a particularly easy determination of the phase position of the maximum pressure. Since the point-glow-discharge lamp of the recording device and the small glow-discharge lamp for the phase indicator have fairly high ignition voltage, some difficulties were encountered at first with the pickup contacts which became overcharged, fouled quickly as a result of carbonized oil, and then formed permanent contact. This was remedied by the tube hookup, figure 4, where the pickup contact has to connect only the grid cut-off bias (30 to 70 volts) and is not charged by current at all.

The test range of the described devices is up to 600-atmosphere positive pressure.

3. Errors.- Since the piston does not run without friction, there is a "frictional error" whose magnitude over the entire test range was statically determined at about ±0.5 atmosphere in a calibration setup. Since the oil-film pressures to be measured are of the order of magnitude of 200 atmospheres and more, this error is of no importance.

A second error termed "acceleration error" is due to the fact that the piston must travel a finite path for which it requires a certain time. As a result, there is an indicator time lag, hence, a distortion of the diagram in the positive direction of the time axis and also a suppression of the indication of very briefly acting extreme pressures. In order to gage the magnitude of this error, some rough calculations

were made while disregarding the damping of the piston motion by the surrounding oil. Table I shows for a 0.16g piston weight and a 0.1-millimeter piston travel, which represents a maximum value, the time (in 10^{-3} seconds and in degree angles at 1000 rpm) which the piston requires to traverse the feed path for various amounts of difference between oil-film pressure and back pressure.

TABLE I.- SWITCHING-ON PERIOD

Δp atmosphere	$s \times 10^{-3}$	Angular degrees at n = 1000 rpm
0.5	0.9	5.4
1	0.64	3.9
2	0.45	2.7
5	0.285	1.7
10	0.202	1.2
100	0.064	0.39

So, whether a short-period pressure peak is still indicated by the apparatus depends upon the duration as well as on the height of the pressure peak. According to this table, for instance, pressure peaks of 0.64×10^{-3} duration are indicated with an error of 1 atmosphere and pressure peaks of 0.2×10^{-3} duration with an error of 10 atmospheres. The distortion of the diagram of an ideal rectangular pressure wave of 10 atmospheres height and 3×10^{-3} seconds duration is represented in figure 5. The wave front is rounded at the upper edge. The sloping back of the wave is probably less changed because the contact itself interrupts on opening at the beginning of the opening process.

Inasmuch as the piston actually moves in oil, the distortions will be even a little greater, but it must be borne in mind that the viscosity of the oil at the operating temperatures of the bearing (60° to 120° C) is no longer high and that the form of the contact and of the piston head had been so chosen that only small quantities of oil are involved.

For a practical test of the reliability of the reading of the oil-pressure gage, a comparison was made with the DVL glow discharge lamp indicator and with the Zeiss-Ikon quartz indicator in such a way that oil-pressure diagrams in the working cylinder of a pulsator were recorded with all three instruments. The pulsator operated at 330 and 1000 rpm; the extreme pressures ranged at about 70 atmospheres. Higher cylinder pressures and speeds were not obtainable with the pulsator. Height and form of the diagrams were found to be practically alike for all three indicators.

Occasionally, the measuring piston had a tendency to stick during operation. Since this was due in part to foreign bodies, a thorough cleaning of the oil is a prerequisite for the success of the measurements. The oil grooves on the piston for better sealing lubrication proved satisfactory. Some of the instruments lasted for more than 50 hours of operations without breakdown.

TESTS AND RESULTS OF MEASUREMENTS

(a) Description of Experimental Setup

The tests were run on a pulsator of the Losenhausen Works, which was installed in the DVL as bearing test rig (fig. 6). The ends of the experimental shaft were supported on roller bearings, the housings of which were attached to the machine bed. The split test bearing is mounted between the two roller bearings. The test bearing can be pressed from below with a constant load against the shaft by means of a worm gear, spindle, helical spring, and guide piston. The compression of the spring is a measure for the applied force. The hydraulic pressure of a controllable constant pressure pump from above acts on the bearing body. An alternating load can be superimposed on this constant pressure by a variable-stroke piston pump. The hydraulic load is indicated strobometrically by a rotary piston on a maximum and minimum pressure gage. By means of this equipment, sinusoidal load reversals up to ±6.5 tons load deflection, eccentric load reversals at the upper brass of from 0 to 13 tons, and constant load at the upper or lower brass up to 15 tons can be produced. Moreover, constant and alternating loads can be superimposed. Load frequency and shaft speed are rigidly coupled by a 1:1 or 1:2 gear, thus insuring one or two shaft revolutions during a load reversal. The number of load reversals is adjustable from 750 to 2200 per minute.

The entire experimental setup is represented in figure 12. In the foreground, at the left, is the back-pressure oil pump with the manometer and the glow discharge lamp for the extreme pressure measurement. A distributor mounted at the pump contains the connections individually closeable by needle valves for the pressure instruments and the diagram-recording apparatus. Oil lines, electrically insulated at the distributor and covered throughout with insulating tubing, lead from these connections to the individual pressure instruments in the test bearing The diagram recorder cannot be seen as it is mounted at the back of the pulsator and rotates with the crankshaft of the alternating load pickup (compare fig. 6). The temperature of the test bearing and of the roller bearings is continuously recorded by a six-color recorder.

(b) Preliminary tests

In the preliminary tests, lead, bronze, and white metal bearings were used, the pressure pickup being mounted in the center of the upper brass (fig. 2). These tests served primarily to check the practical utility of the instrument, although they also produced some interesting results. On one graphitized white metal bearing (No. 54) of 75-millimeter diameter, the extreme pressures shown plotted against the bearing load in figure 7 were measured in the center of the upper brass and disclosed extreme pressures in the oil film up to 515 kilograms per centimeter^2 at that point. The shaft speed was 735 rpm, the number of load reversals the same. The bearing load is expressed as amplitude of the alternating load in tons and as maximum surface pressure referred to the projected bearing surface

$$p = \frac{\text{maximum load } P}{\text{bearing diameter } d \times \text{bearing width } l}$$

The values represented in the upper line were obtained at constant speed, 735 rpm, and variable load. The temperatures in the upper brass varied from $t = 53^\circ$ C at ± 1 ton load to $t = 72^\circ$ C at ± 6 tons load. The values of the lower line were recorded at constant temperature $t = 80^\circ$ C for different loads, the rpm being varied so that the temperature of the brass remained constant. The extreme pressure occurring at the test point in the bearing vertex is, in both cases, approximately proportional to the bearing load. The lubricating oil used in this test was Stanavo 140; in all subsequent tests, Aero Shell medium.

On a lead-bronze bearing (No. 5) with 75-millimeter diameter and 0.045-millimeter radial clearance (difference in radius between bearing and shaft), the extreme pressure curves, shown plotted against the sliding speed (rpm) for different alternating bearing loads in figure 8, were recorded. These values indicate that the pressure at the test point remains fairly constant even at variable sliding speed. The result therefore leads one to suspect that the location of the extreme oil-film pressure, which lies in direction of rotation behind the upper brass center, shifts a little under simultaneous variations of speed and number of load reversals. This suspicion was confirmed by the subsequently described principal tests.

(c) Principal Tests

1. The experimental bearing.- The principal tests for the determination of the oil-pressure distribution were made on a white metal bearing WM 80. Its diameter was 75 millimeters; its effective width, 45 millimeters; the radial installation-bearing clearance, 0.025 millimeters (difference in

radius). The thickness of the supporting shell was 4 millimeters. The pouring thickness was 1 millimeter. The final machining of the bearing was effected on a fine-drill press. The bearing was not scraped again after running-in. The superfinish was not given until after the 22 pressure recorders, with which the bearing was equipped, had been installed. The bearing brass was never removed during the whole test period in order to avoid any subsequent stresses. The bearing had no oil grooves. Seen from the front the oil was fed near the right joint, which, at the same time, was widened out to a small oil pocket. The rotating was counterclockwise, so that the oil reached the upper brass first, then the lower brass. The shaft was of Krupp EFD 70 steel with 115 to 125 kilograms per millimeter^2 tensile strength. Figure 9 represents the upper brass with the 22 test instruments, along with the thermocouple for measuring the shell temperature and the housing of the upper brass with the openings for the test instruments. Figures 10, 10a, and 11 represent two views of the experimental bearing, a diagram of the upper brass with the arrangement of the test stations, and the upper part in assembled condition after a 50-hour running period. Figure 12 is a view of the entire setup. In this experimental bearing the pressure distribution in the oil film of the upper brass was measured at various loads, speeds, and rotational directions.

2. Test results under constant load.- In the constant load tests, the oil-film pressure at the several test points was determined with the glow discharge lamp. The pressure variation in the oil film over one revolution was not recorded in this test, since, under constant load, the pressure in the oil film for the same place remains constant with respect to time.

From these recorded values, the extreme pressure domes can be represented either as model over the developed bearing shell or in form of a family of curves from cross sections and radial sections. The results at constant load are plotted in figures 19 to 19e. Figure 19 represents the pressure distribution over the width of the bearing for different radial sections at 780 rpm and $P = 3$ tons constant load, equivalent to a surface pressure $p = \frac{P}{d \times l}$ of 89 kilograms per centimeter^2. The curves are of parabolic form. The plotting of these and corresponding curves from other tests at logarithmic scale gives the exponent of the curves with 1.9 to 2.2 (reference 1). Figure 19d shows the pressure variation plotted against the developed bearing circumference of the loaded shell. It shows how the bearing pressure rises in direction of rotation, reaches the extreme value shortly aft of the center, and then drops very steeply.

For further interpretation of the test data, the radial section curves were planimetered and an average extreme pressure in the radial section (pm) computed from it and included in figure 19. If these pm values are plotted

as radial rays against a section of the bearing (figure 19a), it results in a representation from which the structure of the pressure peak averaged over the bearing width is readily apparent in the coordinate of the direction of rotation. It should be noted that, for parabolic pressure distribution over the bearing width, the pressure occurring in the center of the bearing shell is in proportion of 3:2 to the pressure averaged over the bearing width. To obtain the pressure in the average cross section from the pm curves of figures 19a and 19c the momentary pm values must be multiplied by 3/2.

From the pm curves, the oil-film pressure p_v acting on the shaft in load direction can be obtained in simple manner. The radially plotted pm lengths are decomposed in vertical and horizontal components, the vertical components plotted against the development of the bearing circumference of the upper brass (fig. 19b) and the resultant area planimetered. Dividing the obtained area by the diameter of the bearing leaves the value p_v referred to the bearing surface $d \times l$. In completely fluid friction, the value p_v should correspond with $p = \frac{P}{d \times l}$. The measurements of the present test gave $p_v = 92$ kilograms per centimeter^2, while $p = 89$ kilograms per centimeter^2. This close agreement is at the same time a satisfactory check on the performed measurements.

In figure 19c the horizontal components of the radial pressure are plotted against the circumference of the bearing. The sum of the forces in this direction are practically equal to zero.

The values represented in figure 19c, which are similar to those in figure 19a, were taken at constant loads of 5 and 6 tons, hence, correspond to an average surface loading of $p = 148$ kilograms per centimeter^2 and 178 kilograms per centimeter^2. The summation of the vertical components of the measured oil-film pressures indicated also a close agreement of the p and p_v values.

During the recording of the oil-film pressures at constant load with the glow discharge lamp, it was noticed, occasionally, that the pressures were not constant, but varied by several atmospheres at a frequency of around 4 seconds^{-1}. The inference from it is that the shaft performs a vibrating motion even under constant load. It might be assumed that these vibrations are introduced by self-excited fluctuations in the structure of the oil film (compare reference 5).

3. Test results for alternating load.- In these tests, the maximum pressure at the several test points was usually determined also with the glow discharge lamp and the test values plotted in radial and cross-section diagrams (figs. 13 and 14). The exponent of the parabolic radial-section curves for alternating load was averaged at 1.8 to 2.2, that is,

equal 2. This result agrees with that by Gümbel-Everling (reference 9, page 54, equation 46) on the theoretical pressure distribution over the bearing width. In many of the tests, the radial-section curves indicated profound dissymmetries (fig. 15) as a consequence of inaccurate mounting, thereby causing the shaft to tilt or cant in the bearing, which was, however, so minute that it could not be identified from starting traces on the surface of the bearing. The dissymmetry of the radial section curves of figure 15 was easily remedied by appropriate layers of paper under the roller bearing blocks supporting the shaft of the test bearing. By this method, a very accurate axially parallel setting of shaft and shell was insured. For example, the effect of a 0.025-millimeter-thick paper shim under a roller bearing could still be distinctly identified. Extrapolating the inclined setting of the shaft by a shim of this thickness, while bearing in mind the roller bearing spacing, to the width of the test bearing, gives a 0.006-millimeter inclined shaft setting referred to total bearing width.

For a simpler and more comprehensive representation of the pressure distribution over the circumference of the bearing, the extreme pressures p_m averaged over the bearing width were again determined from the radial-section curves and plotted against the cross section of the bearing as radial rays. Figures 16, 17, and 18 illustrate such records for various loads, speeds, and rotational directions. The actual extreme pressures in the central cross section of the bearing are here also 3/2 times higher than the corresponding p_m values.

Figure 16 represents the extreme pressures averaged over the bearing width at varying alternating loads of from ±5 tons to ±1 ton as well as at vanishingly small load which could no longer be accurately determined with the test equipment of the pulsator. Speed and number of load reversals were kept constant in this test series (770 rpm). Figure 17 shows three corresponding diagrams for constant alternating load and varying shaft rpm and load reversals (1:1). On comparing the load curves for various speeds, it is found that rise and fall of the pressure dome are so much more rapid as the number of revolutions and load reversals are higher. Because the oil temperatures rose with increasing speed, the oil viscosity itself decreased with increasing speed, so that the steeper rising and falling form of the extreme pressure dome is probably less due to the direct speed effect than to the lower viscosity and the reduced lubricating slit. For the separation of the individual influences of speed, number of load reversals, and viscosity, additional tests are necessary.

The averaged extreme pressure domes of figures 18a and 18b, taken at different direction of rotation of the shaft but equal load and speed, are almost identical. Minor discrepancies are presumably attributable to the ovalization of the bearing and the shaft; besides, the oil inlet remained at the same place and was not shifted in the other joint on reversal of the direction of rotation. In the test in opposite direction

of rotation (fig. 18b), the oil first enters the lower brass and then the upper brass where the test points are located. Curve 18b therefore starts with a pressure value 0 and ends, viewed in direction of rotation, with the value of the feed pressure of the lubricating oil feed, while all diagrams in normal direction of rotation start with this feed pressure and, at the end, decrease to around zero.

A comparison of the average oil-film pressure p_v acting vertically on the shaft with the applied average surface load $p = \frac{P}{d \times l}$ proved the p_v values in all tests at alternating load to be from 10 to 12 higher than in the test at constant load. Since, with fluid friction and simultaneous appearance of the extreme pressures at all test points at the instant of maximum load application at the bearing, the value p_v must be equal to the value p, while at semifluid friction (where, aside from the oil film, the metal surfaces in direct contact are also contributing,) only lower values for p_v than for p are to be expected; the only likely cause for the two high p_v values appeared to be a time-phase displacement of the extreme pressures in the oil film.

This was confirmed by the time-pressure diagrams taken at each test point. Figures 20 and 21 represent several such diagrams obtained at $P = \pm 3$ tons alternating load ($p = 89$ kilograms per centimeter^2), 770 rpm and 1:1 gear ratio. The phase shift is readily apparent in a comparison of the different diagrams. The evaluation of these pressure records afforded the curve I of figure 22, where the time-phase displacement of the extreme pressures at the individual test points is indicated with respect to the instant of maximum load acting at the bearing (angle in degrees referred to a complete load cycle).

While the apparent phase differences are not very great, especially in the area of the very highly loaded test points, they are still sufficient to explain the differences between p and p_v. The phase displacement is attributable to the motion of the shaft in the bearing by which the location of the minimum film thickness is displaced during a load alternation. Since no equipment for recording the shaft motion in the bearing was available, certain deductions from figure 22 must suffice for the time being. At start of the loading of the upper brass, the minimum film thickness is presumably near the test points 20 to 22 (figure 23). As the load increases, it travels over test points 15, 11, and 7, which it reaches late with respect to the moment of maximum load. In consequence, the shaft center moves probably fairly rapidly toward test point 1. This process is repeated in the lower brass. Such a motion of the center shaft on an approximately obliquely lying ellipse or on an open figure of eight relative to the direction of shaft rotation would explain the phase shifts and several peculiarities of the forms in figures 20 and 21. Thus, the expreme pressure in the oil film occurred

at the test points 20 to 22 about 50° angle shaft rotation ahead of the instant of outwardly applied maximum load on the bearing (compare instrument 21, figure 21). Moreover, the diagrams were very short. The maximum pressure in the oil film at these test points is mainly caused by the passage of the narrowest bearing clearance at start of the load reversal process, while, at the instant of maximum load, these test points lie already considerably behind the minimum film thickness and have only a rather low pressure at this instant. For test points 17 to 19, the lead of the extreme oil-film pressure over the maximum load is no more than about 35°. At test points 13 to 16, the effects of the gradually widened slit and the increasing load of longer period neutralize each other so that the diagrams obtain an elongated form flattened at the top, while at test points 10 to 12, the minimum film thickness and, hence, the extreme pressure already occurs distinctly late (instruments 15 and 11, figure 21); at the instant of maximum load the minimum film thickness should accordingly lie between points 13 to 16 and 10 to 12. The rapid decrease of the diagram from instrument 11 is attributable to the decrease in load with contemporary jumping of the shaft toward test point 1, hence, where two pressure reducing effects are additive. At test points 3 to 9, the maximum pressure in the oil film is practically simultaneous with the maximum load, which is indicative of the fact that the shaft in its motion misses these test points, so to speak, hence that no substantial slit contractions occur here and that the maximum pressures in the oil film are principally dependent upon the bearing load only (instruments 5 and 7, figure 20). The diagrams of test points 1 and 2, which disclose two peaks, can then be explained such that the first peaks, which approximately appear at the instant of maximum load, are caused by the maximum load, and the second peaks, established 80° and 90° after maximum load, are due to the shaft displacement (instrument 1, figure 20).

From these considerations it was attempted, in figure 22, to identify curve II, the probable momentary position of the minimum film thickness in the bearing shell as phase displacement with respect to the instant of maximum load acting on the bearing from the outside. The entry of the minimum film thickness in the upper brass occurs accordingly about 70° ahead of the maximum load at the joint lying to the rear in direction of rotation. By the time the maximum film pressure for test points 20 to 22 appears (approximately 50° before maximum load), the minimum film thickness itself will be at this place. At the instant of maximum load, the minimum film thickness should be between test points 13 to 16 and 10 to 12 and 80° and 90°, respectively, after maximum load reach test points 1 and 2 (at the appearance of the second maximum in the oil film pressure diagram). About 110° after the moment of maximum load, the minimum film thickness would leave the upper brass. The entire stay of the minimum film thickness in the upper brass would then extend to 180° shaft rotation angles and repeat itself correspondingly in the lower brass.

A form similar to that of the shaft motion deduced in figure 23 is obtained when proceeding from the theoretical semicircular path of the shaft center at slowly increasing load (steady). It likewise gives an obliquely placed ellipsoidal path or an open figure eight as shaft center path for alternating load. However, this supposition requires exact experimental proof. For very high loads at incipient semifluid friction the conditions are different, as will be explained later.

A comparison of the test data at constant and alternating load indicates a smoother rise and fall of the pressure curves in the cross-sectional representation for constant load. This is entirely logical, since at constant load the pressure is solely built up by the rotation of the shaft and the effects of the shaft motion under alternating load do not exist.

4. Transition to semifluid friction under alternating load.- According to figures 16 and 17, the location of the absolute maximum pressure appears, for the first, to be little affected by the speed and load. It remains at about the same place on the circumference near test instrument 11, 16° behind the bearing vertex, so long as the bearing load does not exceed a certain limit value, which, at 770 rpm, lies at about ±6 tons on the explored bearing. If the load is increased further the shape of the pressure dome is radically changed. In figure 24 the cross-section curves through the averaged maximum pressure dome are represented at ±5 ton, ±6 ton, $^{+7}_{-5.4}$ ton and $^{+8}_{-4.3}$ ton loads for 775 rpm. (In the last two tests, the upper and lower brass could not be loaded identically, because of inadequate pulsator equipment. For this reason, only the upper brass was subjected to a 7 and 8 ton maximum load, although this should alter the results very little).

At loads above 6 tons, the peak of the pressure dome travels in direction of instruments 4 and 5, which are located in front of the bearing center (74° at circumference of bearing). This phenomenon can be explained by the appearance of semifluid friction at the high loads, where shaft and bearing (with their surface roughness) come in contact with each other. The result is a rolling-down motion of the shaft in the bearing opposite to the direction of rotation, through which the narrowest bearing slit then appears before the bearing center. Simultaneously, the height of the pressure dome at increased load beyond the limiting load for fluid friction does no longer increase in proportion to the load increase, because then forces are transmitted by the direct contact of shaft and bearing. This naturally changes the path of the shaft center of figure 23 considerably. It would have to assume a form for which the narrowest slot in contrast to that shown in figure 23 is shifted from the vertical toward the right and upward.

For the load still permissible at the boundary between fluid and semifluid friction, E. Schneider (reference 2) has quoted a minimum value for the expression $\frac{\eta \times n}{p}$ with respect to the corresponding bearing clearance $\frac{R - r}{r}$ and the bearing diameter d, below which it must not fall, to avoid disturbances (η = viscosity). Applying this relation as a check on the present test data for 775 rpm (figure 24), gives, in accord with the result achieved by the oil film pressure measurement, a load limit of about p = 180 kilograms per centimeter^2 for fluid friction. The same characteristic variation of the pressure dome occurs also at higher speed (2000 rpm) and corresponding load $\left(\begin{matrix}+7.5\\-5.5\end{matrix}\text{ tons and }\begin{matrix}+8.1\\-5.5\end{matrix}\text{ tons}\right)$ according to figure 25. The fact that the load capacity of the oil film is not greater than in the previous tests despite the higher speed is also likely to be due to the higher temperature and the concomitant lower viscosity of the oil (reference 10). A comparison of the $\frac{\eta \times n}{p}$ values for an 8-ton bearing load at 775 and 2000 rpm, η to be inserted in correspondence with the particular temperatures (75 or 110°), indicates that the product $\eta \times n$ at both speeds is practically the same. Thus the measurement of the oil film pressure dome of a bearing at progressively increasing constant or alternating load is a practical means for the determination of the load limit, where fluid friction changes to semifluid friction.

On the bearings tested so far on the pulsator test rig for fatigue strength, the destructive phenomena (crumbling, porosity, and cracks) usually appeared first behind the bearing vertex in the area of test station 11. These bearings ran therefore probably for the most part in the zone of fluid friction. The high alternating oil pressure resulted in fatigue and consequent crushing of the material.

(d) Scope of tests - application of results

The present experiments, made primarily within the framework of testing an oil film pressure apparatus, indicate that even this single test equipment affords a close insight into all the details of the oil film formation in the journal bearing. It was found to be absolutely necessary to record the motion of the shaft center in the bearing accurately, because the motion processes deduced from the pressure measurements can give only an approximate picture of the actual setting of the shaft. On top of that, the behavior of the oil film at transition to high loads must also be accurately followed up. At the highest oil film pressures of 600 atmospheres recorded in the test bearing, the relationship of oil viscosity and pressure established by Kiessalt (references 11, 12, and 13) as well as the dynamic viscosity of thin lubricating films ascertained by Kyropoulos (references 14

and 15) are no longer negligible and must be taken into consideration for the evaluation of the load capacity of the bearing.

Along with the present pressure recording a number of insulation measurements by oscillograph were conducted between bearing shell and shaft, although it was found that this method alone was insufficient for an acceptable prediction of the transition from fluid to semi-fluid friction. In many instances very minute metal particles in the oil or the touching of a few tiny surface particles, which practically can have no effect on the load capacity of the bearing, were sufficient to almost cause a short circuit between bearing and shaft. In any case, the limit of the load capacity of an oil film can be more definitely established by measuring the oil film pressure, and in certain conditions the same method might even be utilized for the evaluation of lubricating oils in practical operation.

The destructive phenomena such as cracking or becoming porous observed in the area of maximum oil film pressure at fluid friction make it seem likely that perhaps the pulsating oil pressure itself, which acts on a bearing metal surface, can create such surface destructions even without supervenient friction, bending stresses, and so forth. Probably the oil, which has penetrated the fine pores of the metal, increases and decreases its volume continuously during the repeated pressure variations, which were measured up to 600 atmospheres, and thus wear down the structure from within.

Translated by J. Vanier
National Advisory Committee
for Aeronautics

REFERENCES

1. Nücker, W.: Über den Schmiervorgang im Gleitlager. Forsch. Arb. Ing.-Wes. Nr. 352 (1932).

2. Schneider, E.: Versuche über die Reibung in Gleit- und Rollenlagern. Petroleum Bd. 26 (1930), pp. 221-236 and 337-348.

3. Vieweg, V., and Kluge, I.: Über Messungen der Schmierfähigkeit von Ölen in Lagern. Arch. Eisenhüttenwes. Bd. 2 (1929), pp. 805-811.

4. Wolff, R.: Über die Schmierschicht in Gleitlagern und ihre Messung durch Interferenz. Forsch.-Arb. Ing.-Wes. Nr. 308 (1928).

5. Hummel, C.: Kritische Drehzahlen als Folge der Nachgiebigkeit des Schmiermittels im Lager. Forsch.-Arb. Ing.-Wes. Nr. 287 (1926).

6. Hein, Piet.: Experimentelle Untersuchung der Grenzbedingungen flüssiger Reibung im oszillierend belasteten Gleitlager. Petroleum Bd. 28 (1932), Nr. 19.

7. Brandt, R., and Viehmann, H.: Der DVL-Glimmlampen-Indikator für schnellaufende Motoren. 322. Bericht der DVL, Berlin-Adlershof, A.T.Z. Bd. 36 (1933), Nr. 12 pp. 309-311.

8. Schmidt, F.: Ein neuer Indikator für schnellaufende Motoren. Z. VDI Bd. 77 (1933), Nr. 27.

9. Gümbel-Everling: Reibung und Schmierung im Maschinenbau. Verlag M. Krayn (1925).

10. Falz, E.: Grundzüge der Schmiertechnik. 2. Auflage (1931), Verlag Springer.

11. Kiesskalt, S.: Untersuchungen über den Einfluss des Druckes auf die Zähigkeit von Ölen und seine Bedeutung für die Schmiertechnik. Forsch.-Arb. Ing.-Wes. Heft 291 (1927).

12. Kiesskalt, S.: Neuere Ergebnisse über die Druckzähigkeit von Ölen. Z. VDI Bd. 73 (1929), Nr. 42, pp. 1502-1503.

13. Kiesskalt, S.: Die Erscheinungen der Lagerreibung und Schmierung. Handbuch der Experimentalphysik Bd. 4, 2. Teil.

14. Kyropoulos, S.: Schmiermittelreibung und Strömungsorientierung. Z. techn. Physik Bd. 10 (1929), Nr. 2, p. 46.

15. Kyropoulos, S., and Schobert: Ein einfaches Verfahren zur Bestimmung des nicht viskosen Reibungskoeffizienten dünner Schmierschichten. Ing. Arch. Bd. 7 (1936), Nr. 4, pp. 222-228.

16. Donandt, H.: Über den Stand unserer Kenntnisse in der Frage der Grenzschmierung. Z. VDI Bd. 80 (1936), Nr. 27, p. 821.

17. Heidebroek, E.: Zur Theorie der Flüssigkeitsreibung zwischen Gleit- und Wälzflächen. Ing.-Wes. Bd. 6, Nr. 4.

18. Rüchardt, E.: Grösse und Masse der Moleküle und Atome. Deutsches Museum. Abhandlungen und Berichte. Heft 1, VDI-Verlag. (Aufbau von Ölmolekülen und Verhalten dünner Schmierschichten.)

19. Rotzoll, E.: Untersuchungen an einem Gleitlager für die Hauptspindel von Feinbearbeitungsmaschinen. Z. VDI Bd. 80 (1936), Nr. 27, p. 821.

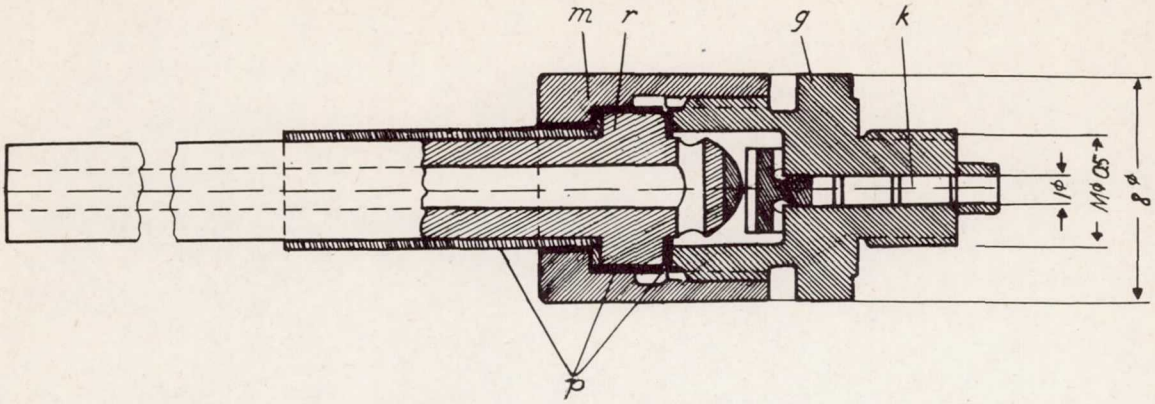

Figure 1.- Pickup for oil film pressure recording device.

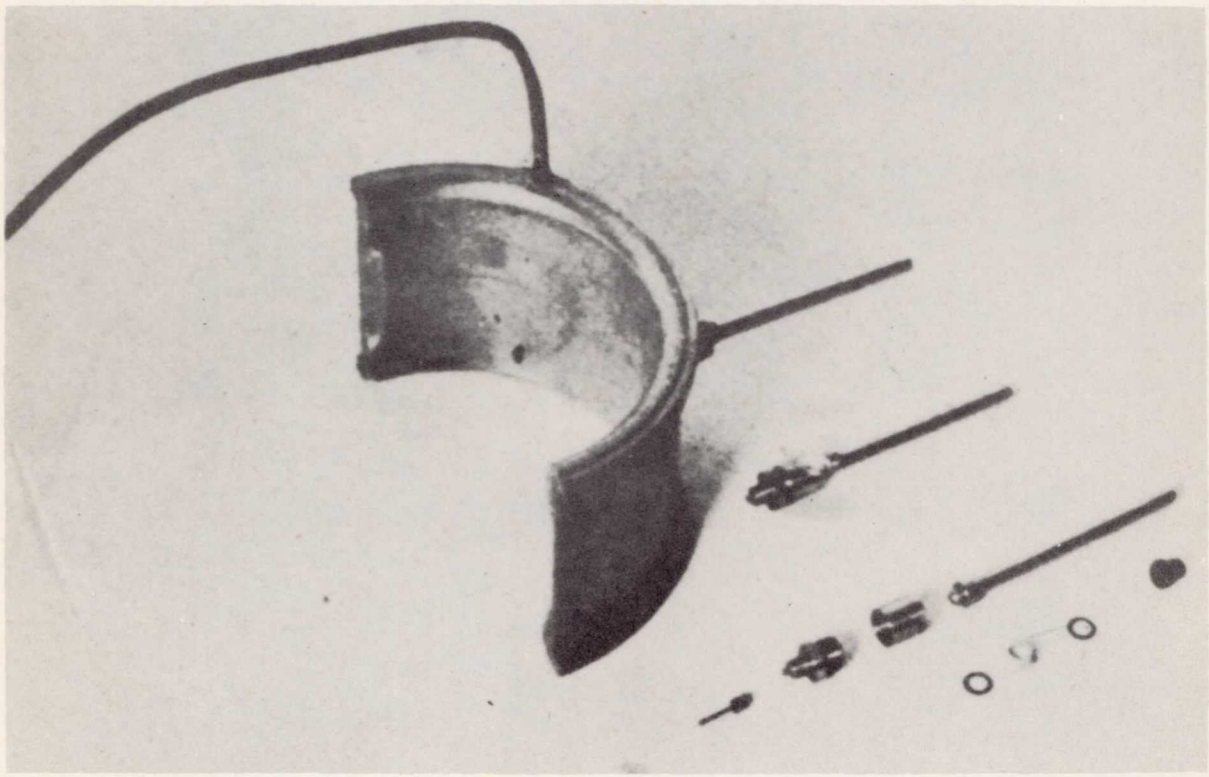

Figure 2.- Pickup for oil film pressure recording device showing exploded view, assembled and mounted in bearing shell.

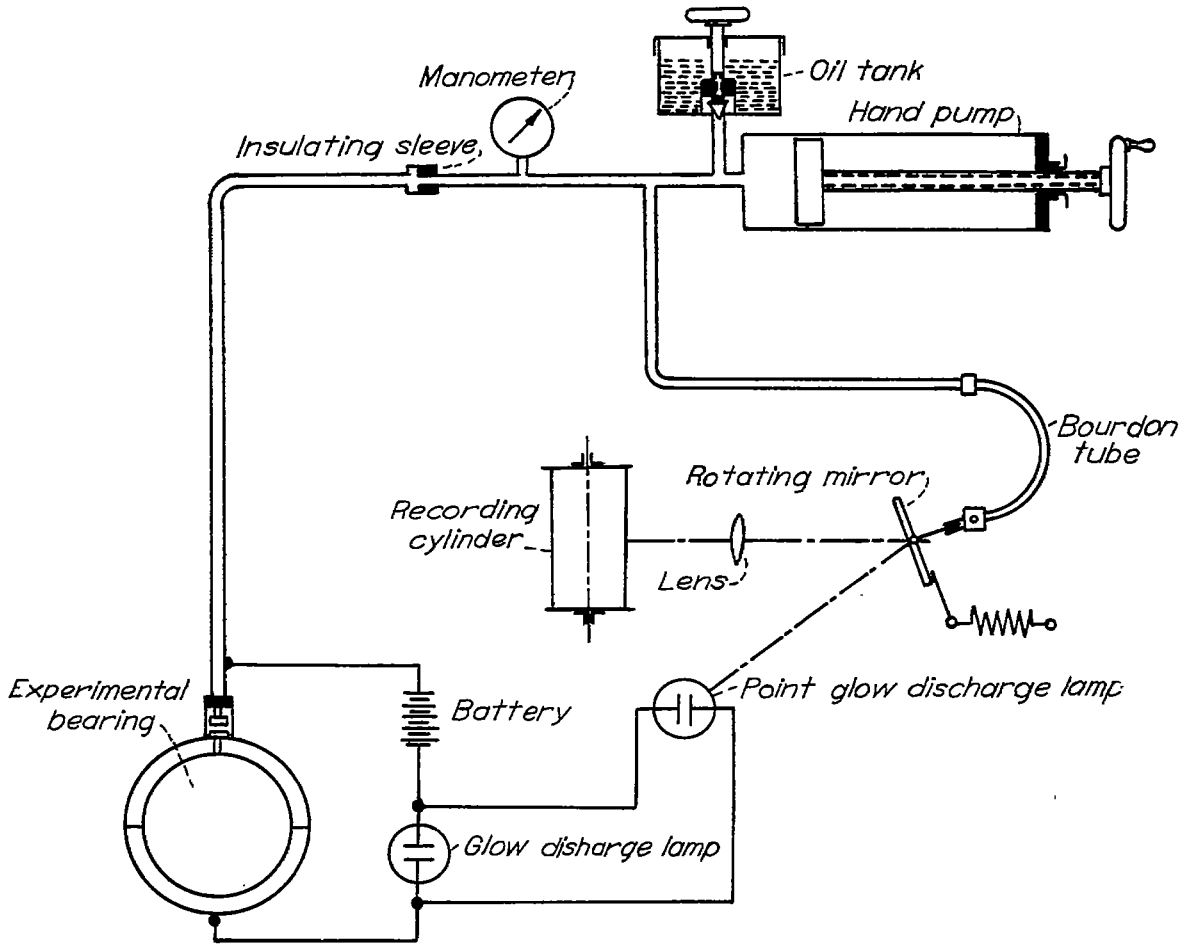

Figure 3.- Indicating equipment for oil film pressure recording device.

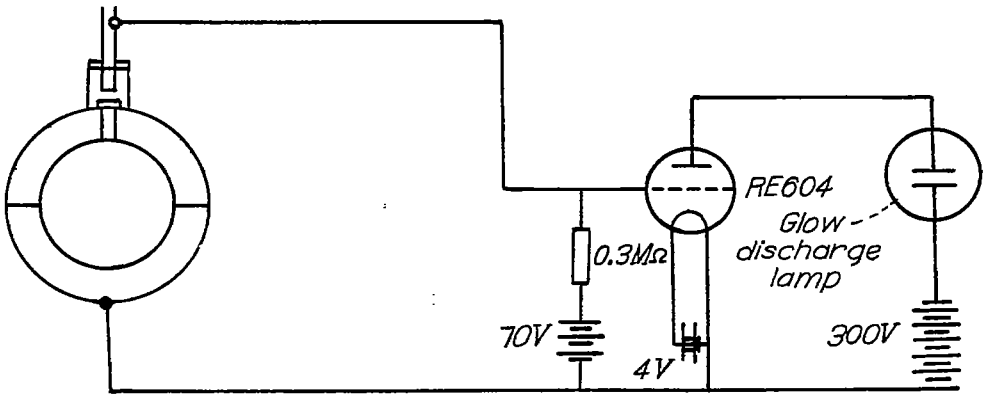

Figure 4.- Wiring diagram for the glow-discharge lamp.

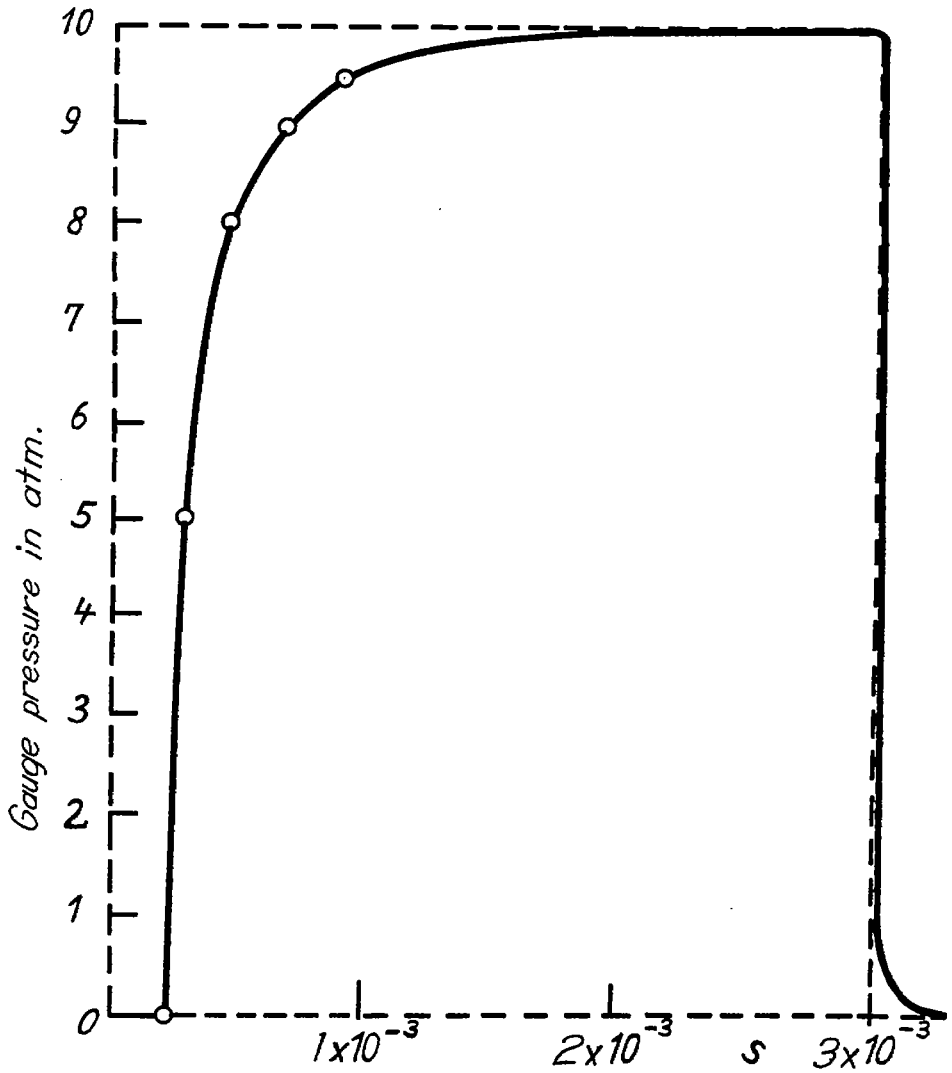

Figure 5.- Distortion of rectangular pressure wave of 10 atmospheres height and 3×10^{-3} seconds duration.

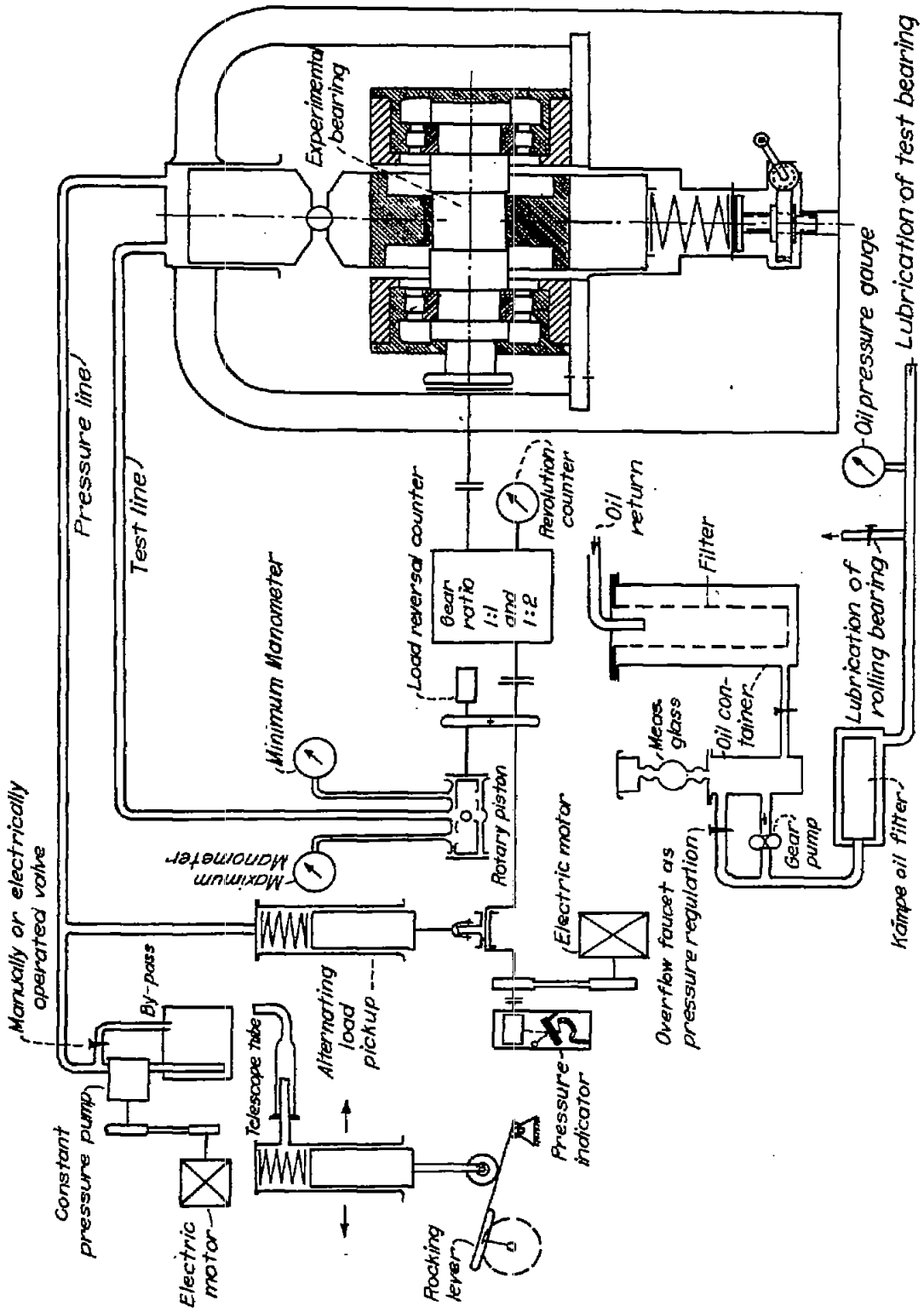

Figure 6.- View of the pulsator-bearing testing machine.

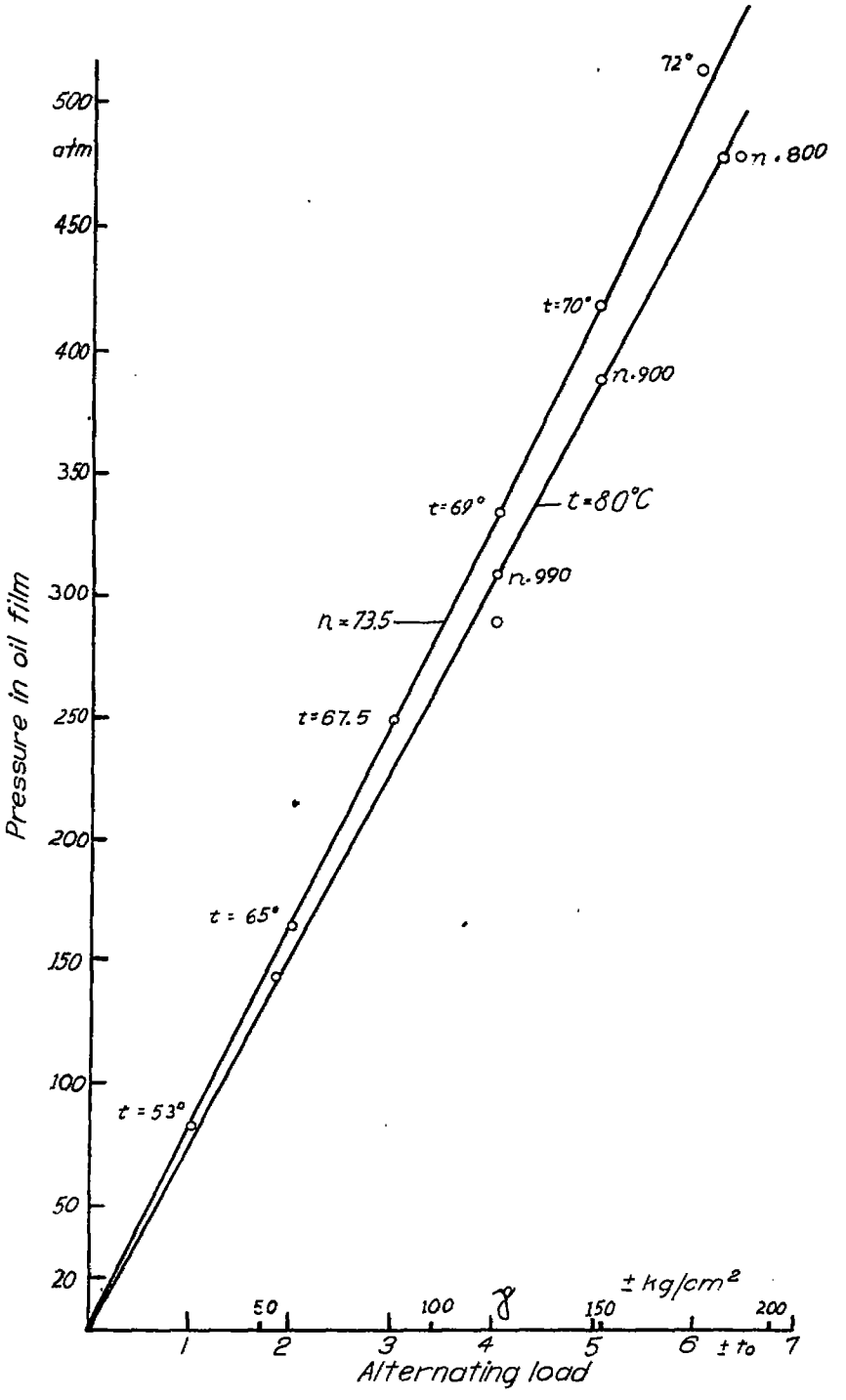

Figure 7.- Maximum pressure in oil film, measured in the vertex of the graphitized white metal bearing No. 54.
Shaft: Krupp EFD 70 No. 3
Lubricant: Stanovo 140
Radial bearing clearance 0.04 (mm) radii difference
Gear ratio: load reversal: rpm = 1:1

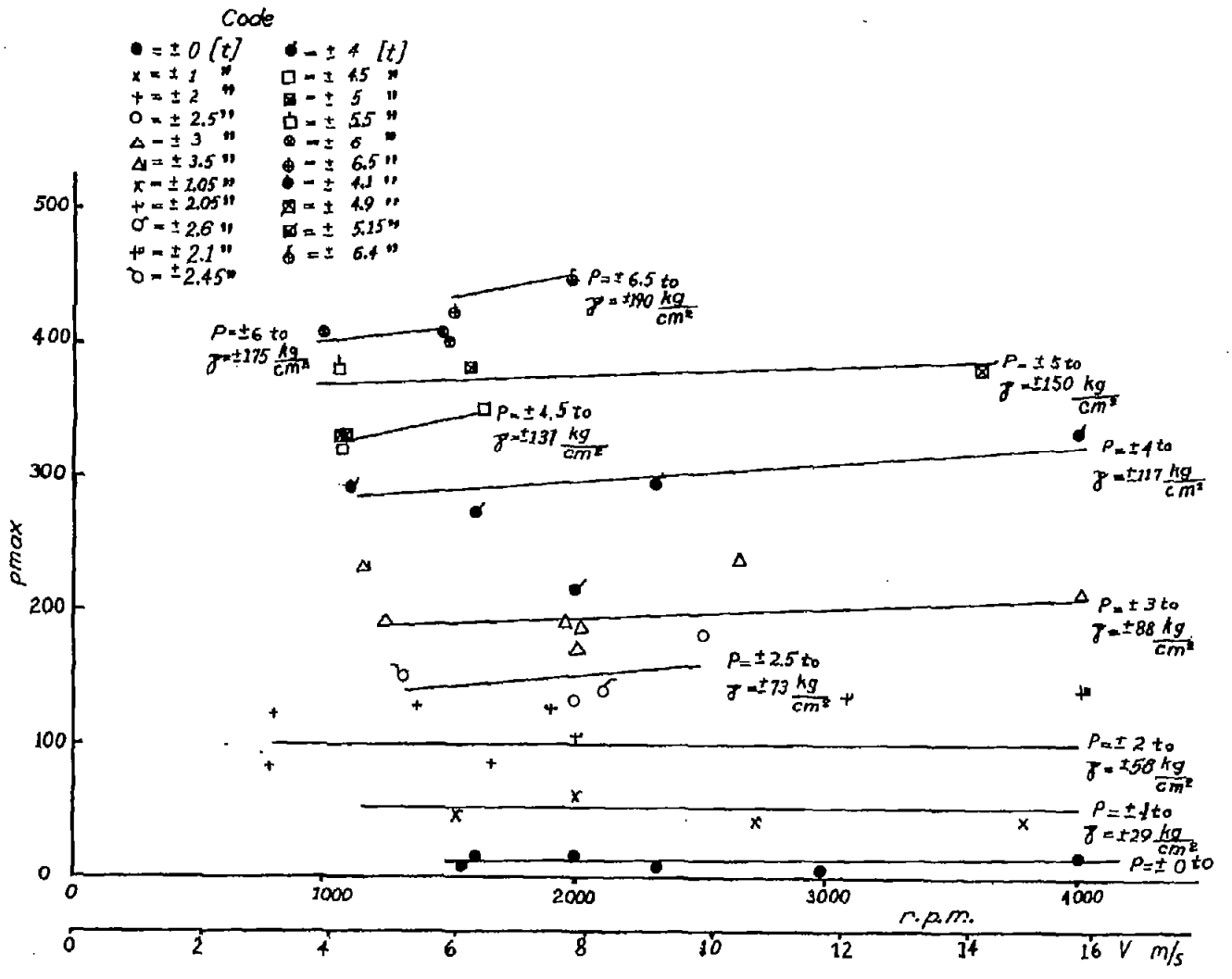

Figure 8.- Maximum pressure in oil film, measured in the vertex of lead-bronze bearing No. 5.
Shaft: Krupp EFD 70 No. 3
Lubricant: Aero Shell, medium
Bearing temperature: 80....150° C
Radial clearance 0.045-mm radii difference

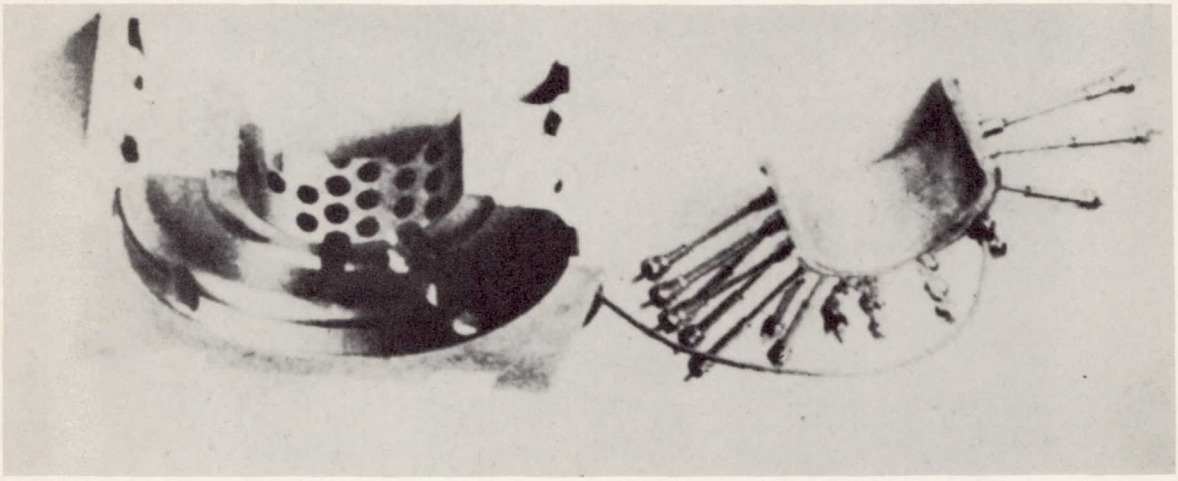

Figure 9.- Experimental bushing and bearing housing.

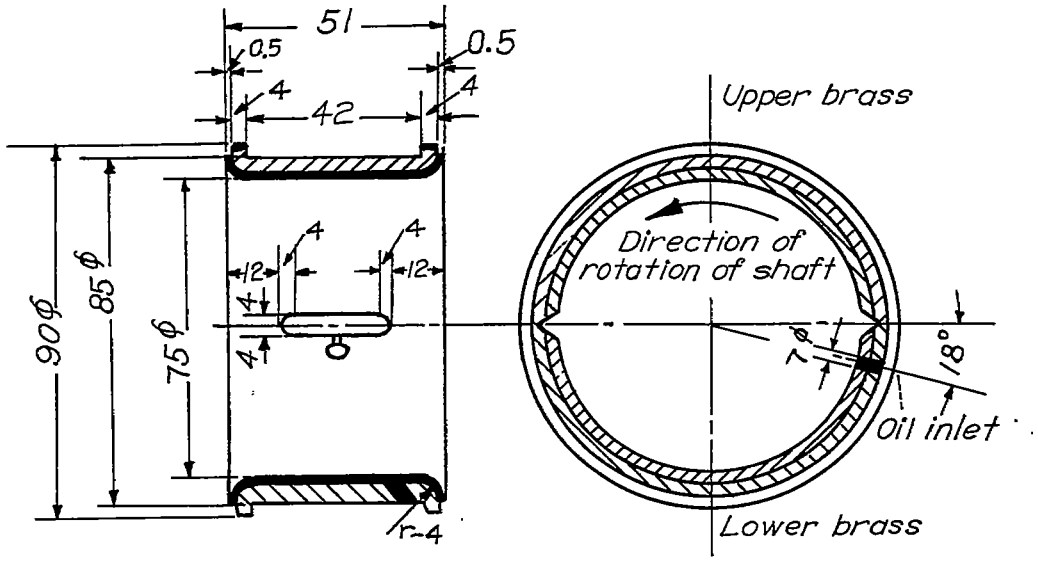

Figure 10.- Dimensions of test bearing.

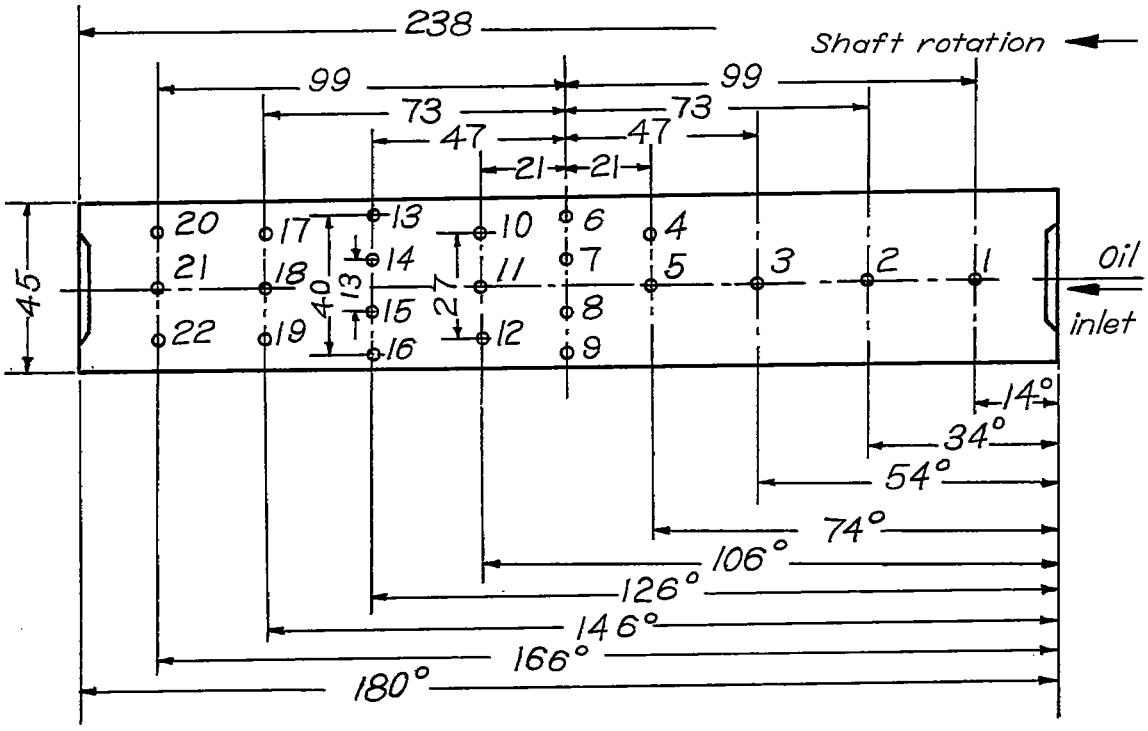

Figure 10a.- Position and identification of test points in the development of the upper brass.

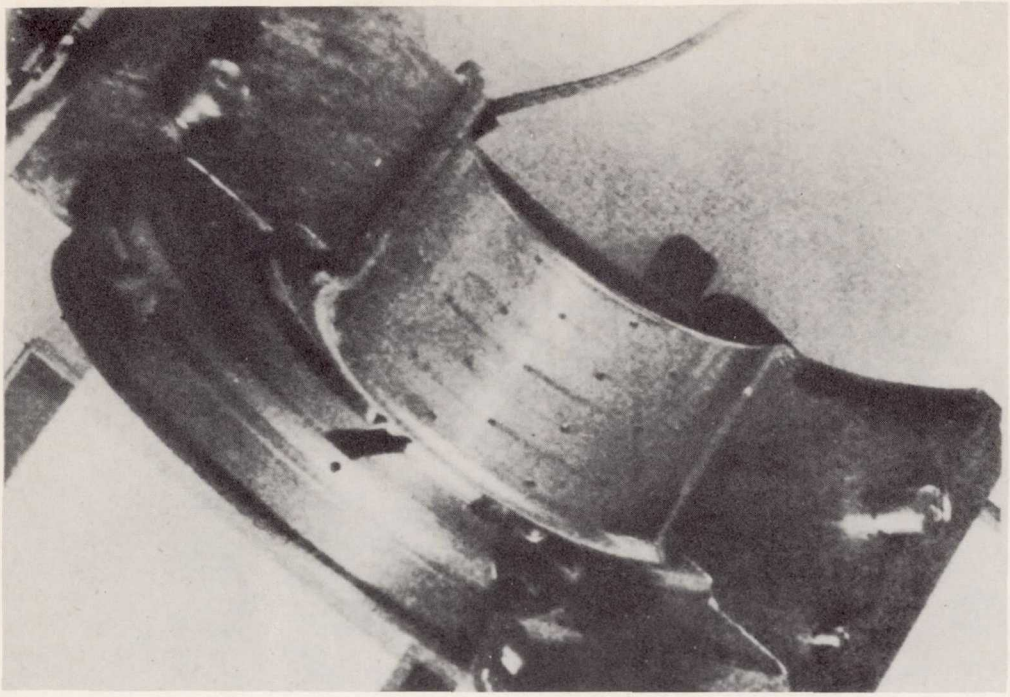

Figure 11.- Upper part of test bearing after 50 hours of operation.

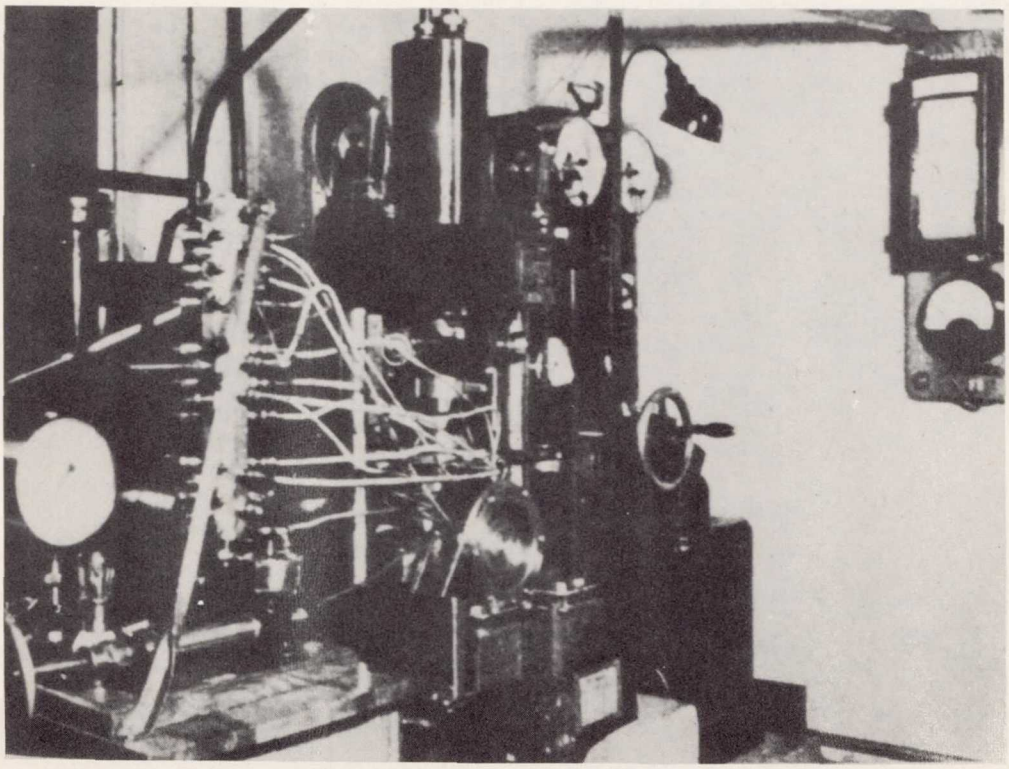

Figure 12.- View of entire experimental setup.

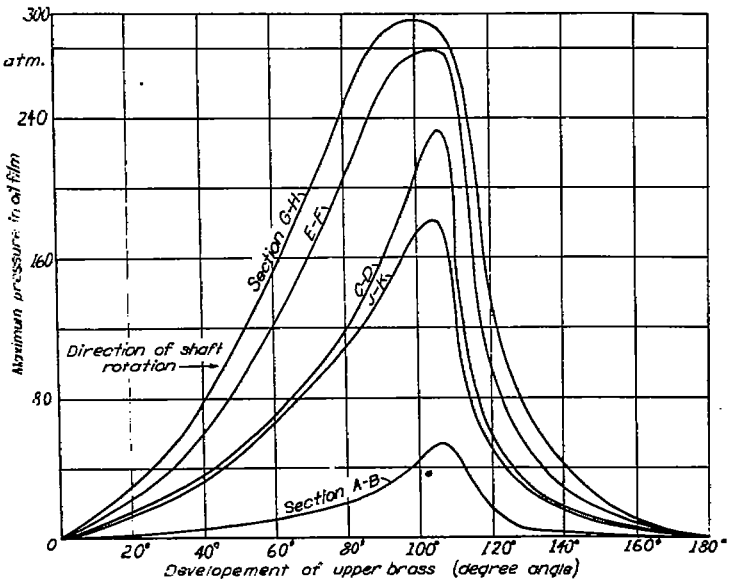

Figure 13.- Maximum oil film pressure plotted against the developed bearing circumference of the upper brass for the different cross sections of figure 14.

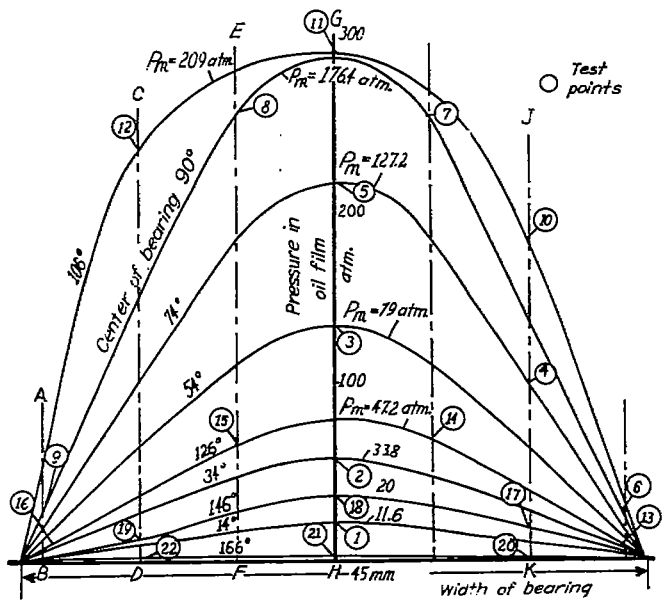

Figure 14.- Radial cuts through the maximum pressure dome below the circumferential angles of 14°, 34°, 54°, 74°, 90°, 106°, 126°, 146°, and 166°.

White metal bearing No. 06
Oil pump pressure: 8 atmospheres
Speed: 760 rpm
Gear ratio 1:1
Load ± 3 tons (p = 89 kg/cm²)
Temperature t = 70° C

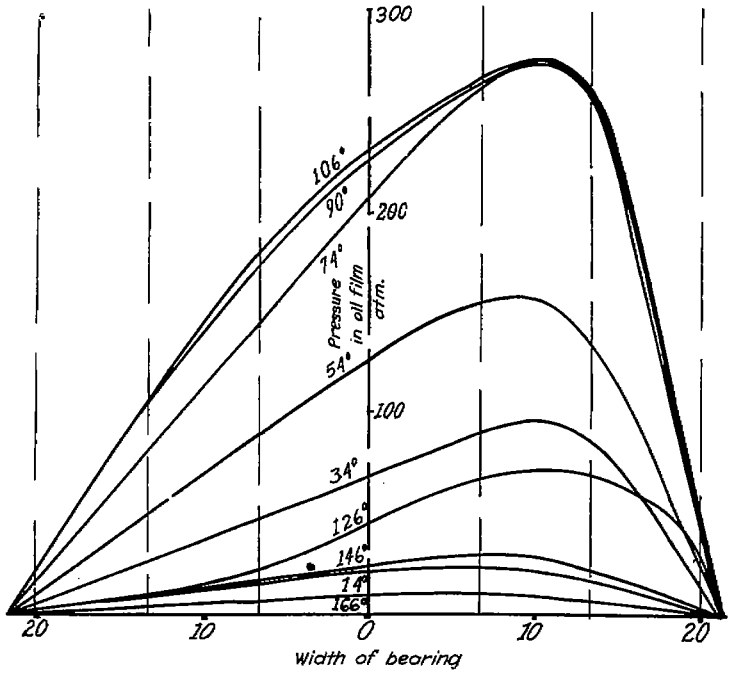

Figure 15.- Radial cuts through the maximum pressure dome at inclined position of shaft in bearing.
Oil pump pressure 6 atmospheres
Speed: 800 rpm
Gear ratio: 1:1
Load ± 3 tons (p = 89 kg/cm^2)
Temperature t = 70° C

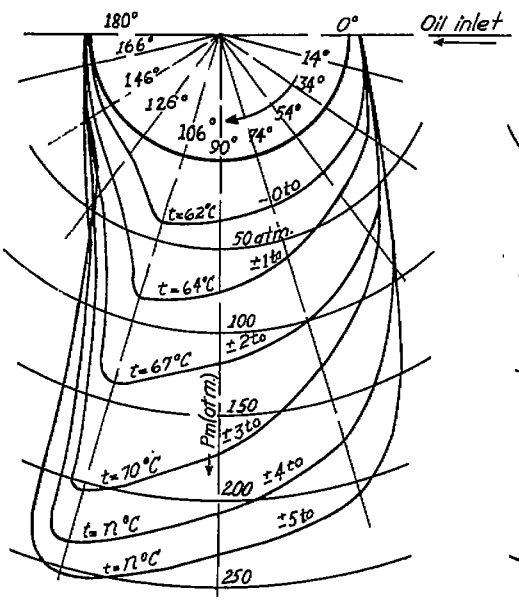

Figure 16.- Bearing cross section with maximum pressures p_m averaged over the bearing width for different loads at 770 rpm.

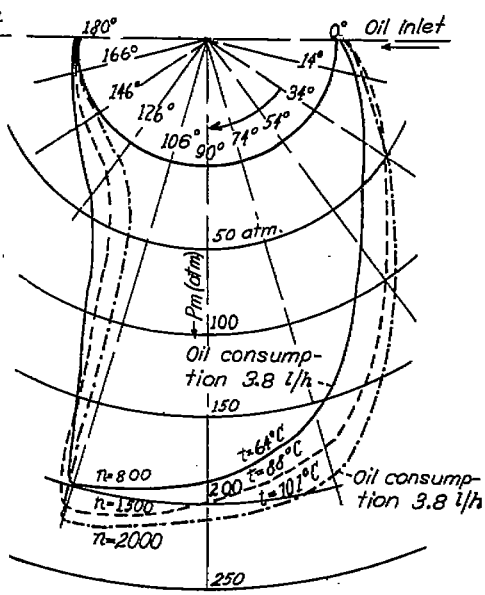

Figure 17.- Bearing cross section for load ± 3 ton (p = 89 kg/cm^2) at different rpm.
Oil feed pressure: 6 atmospheres
Gear ratio: 1:1
Room temperature: 23° C

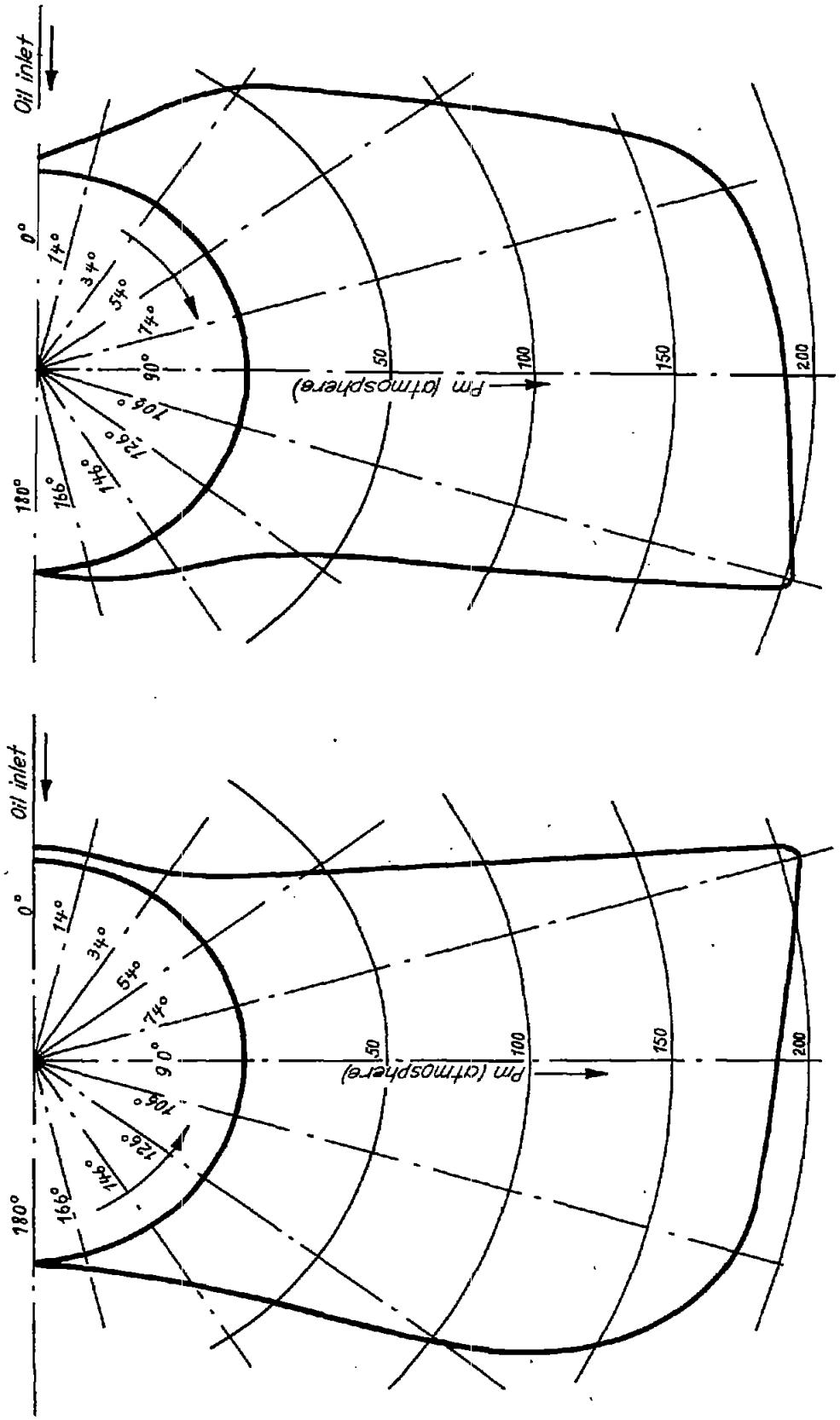

Figure 18.- Bearing cross section with maximum pressure p_m averaged over bearing width for different direction of rotation at equal load and speed.

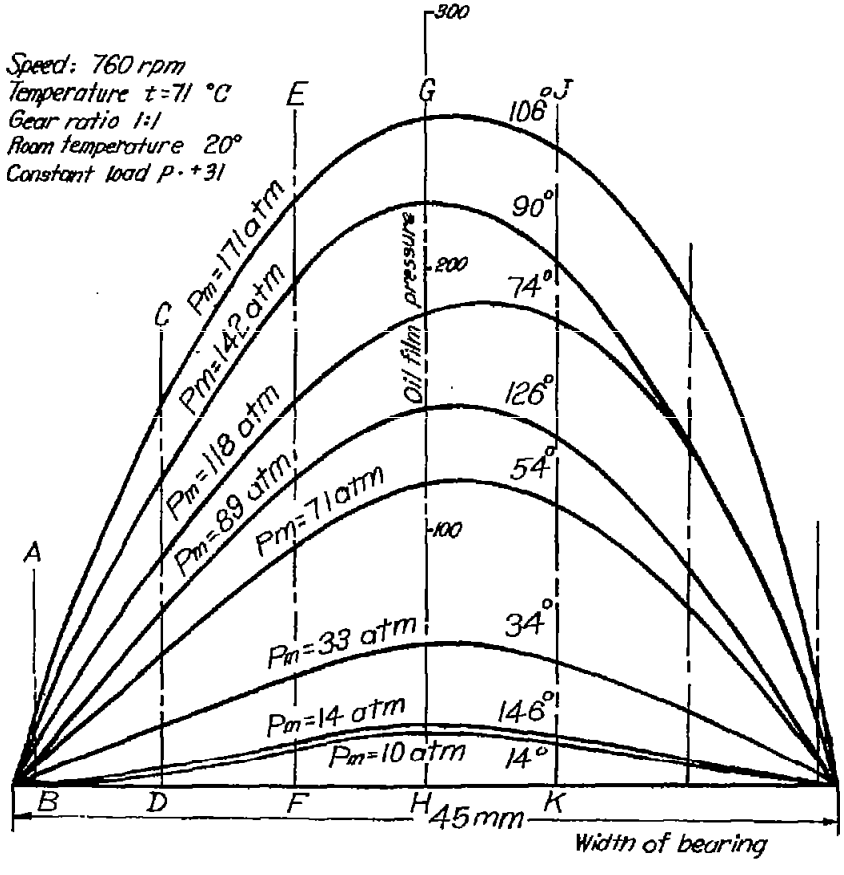

Figure 19.- Radial cuts normal to bearing width in the plane 14°, 34°, 54°, 74°, 90°, 106°, 126°, 146°, 166° of the bearing circumference; oil feed pressure 6 atmospheres.

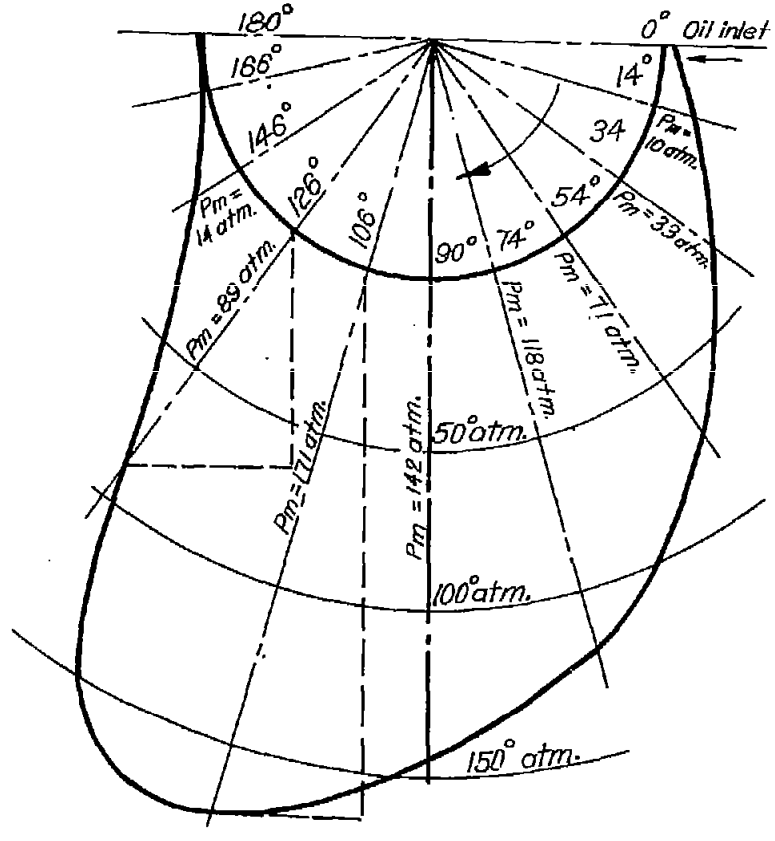

Figure 19a.- Bearing cross section with film pressure p_m averaged over bearing width.

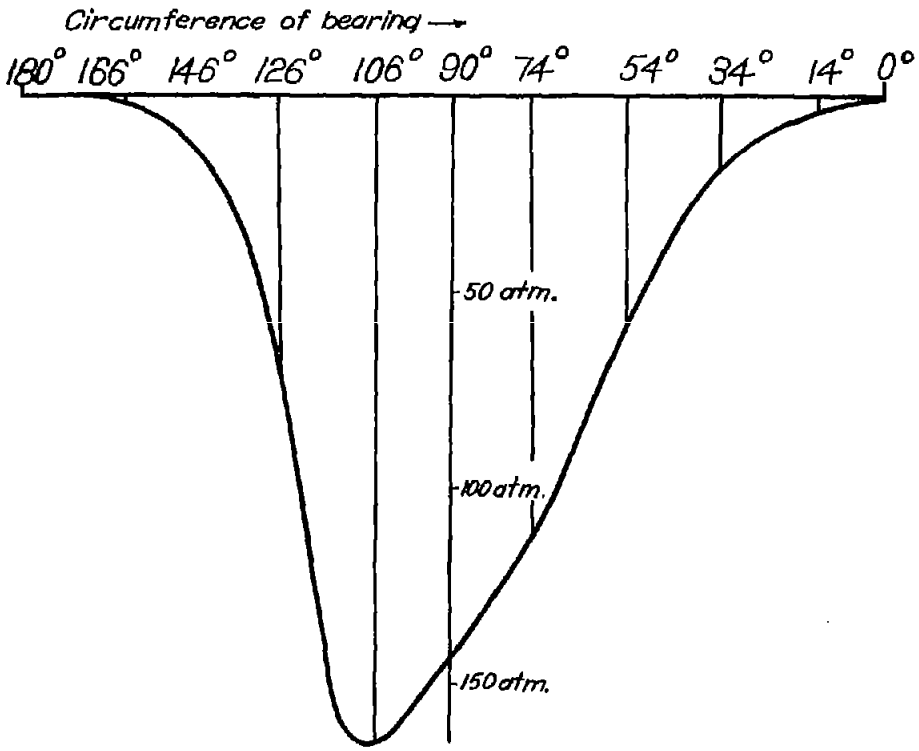

Figure 19b.- Vertical components of the film pressure p_m averaged over the bearing width plotted against the developed upper brass.

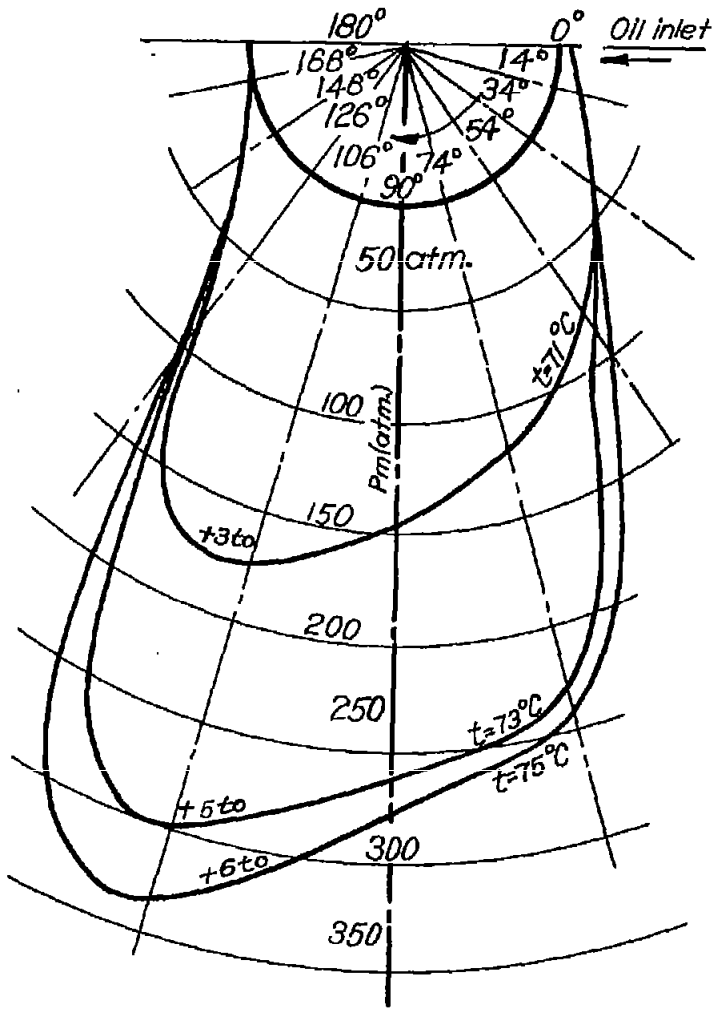

Figure 19c.- Bearing cross section with oil film pressure p_m averaged over bearing width for various constant loads at constant speed of 780 rpm; gear ratio: 1:1, room temperature = 21° C, oil feed pressure = 6 atmospheres.

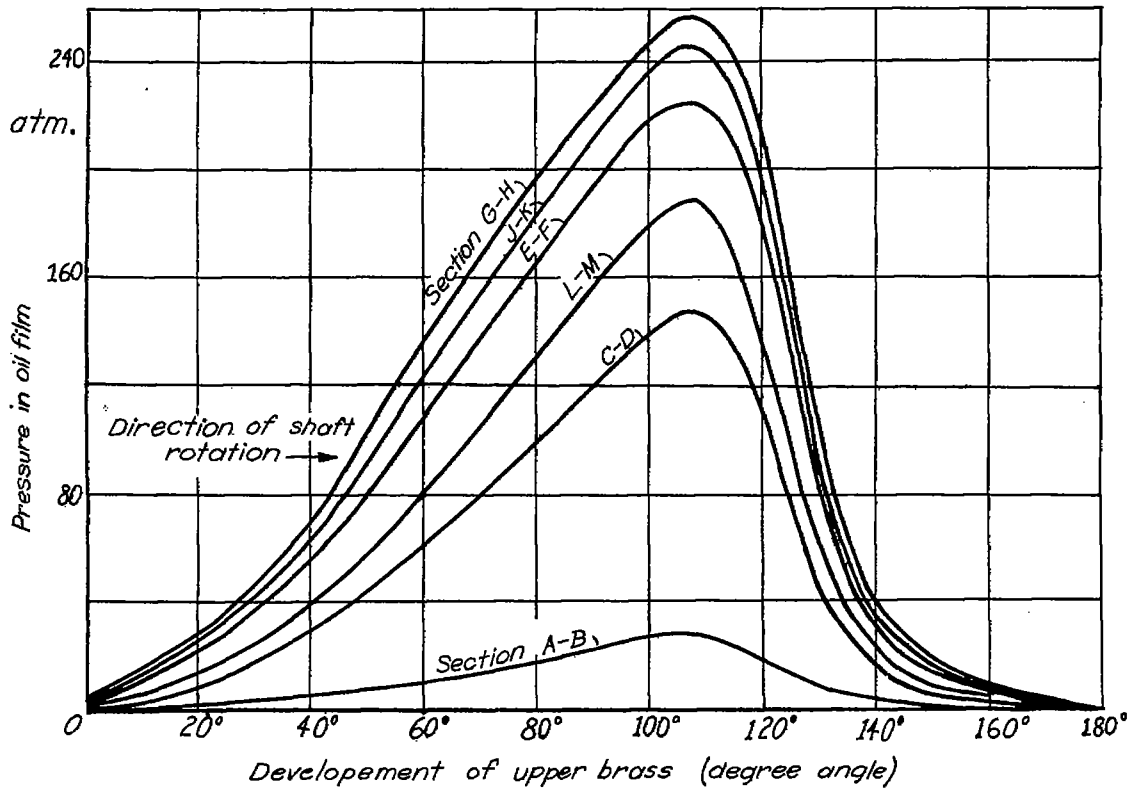

Figure 19d.- Oil film pressure variation plotted against the developed bearing circumference of the upper brass for various cross sections of figure 19.

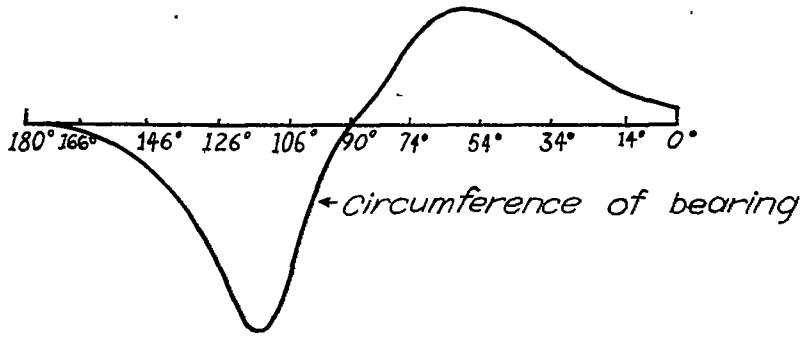

Figure 19e.- Horizontal components of the radial pressures of figure 19a.

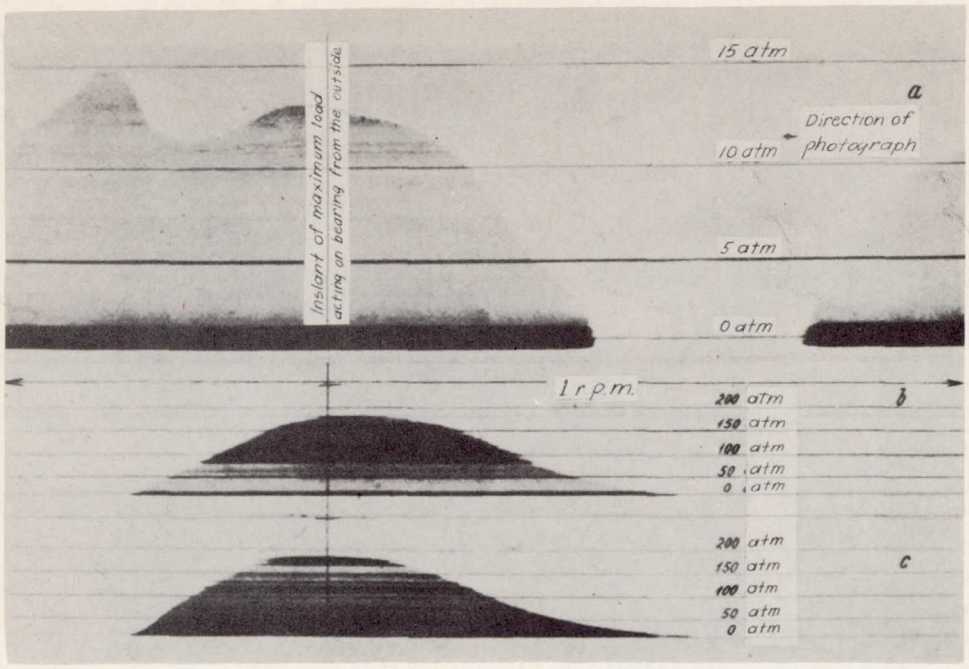

Figure 20a.- Instrument 1. p_{max} ~ 14.5 atm. Weak spring record.

b.- Instrument 5. p_{max} ~ 180 atm. Strong spring record.

c.- Instrument 7. p_{max} ~ 185 atm.

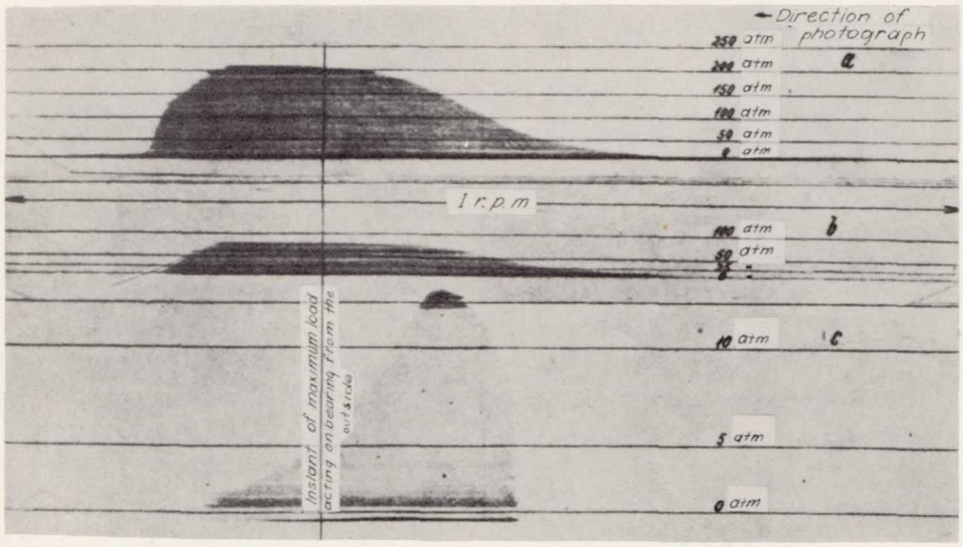

Figure 21a.- Instrument 11. p_{max} ~ 220 atm.

b.- Instrument 15. p_{max} ~ 80 atm.

c.- Instrument 21. p_{max} ~ 12.5 atm. Weak spring record.

Figure 20 and 21.- Pressure variation in oil film over 1 revolution at the various test points.

Load ±3 tons
Load reversal 1/770 rpm
Gear ratio 1:1
Bearing shell temperature 71° C

Radial clearance 0.025 mm
Oil pressure 6 atmospheres
Oil consumption 3.3 l/h

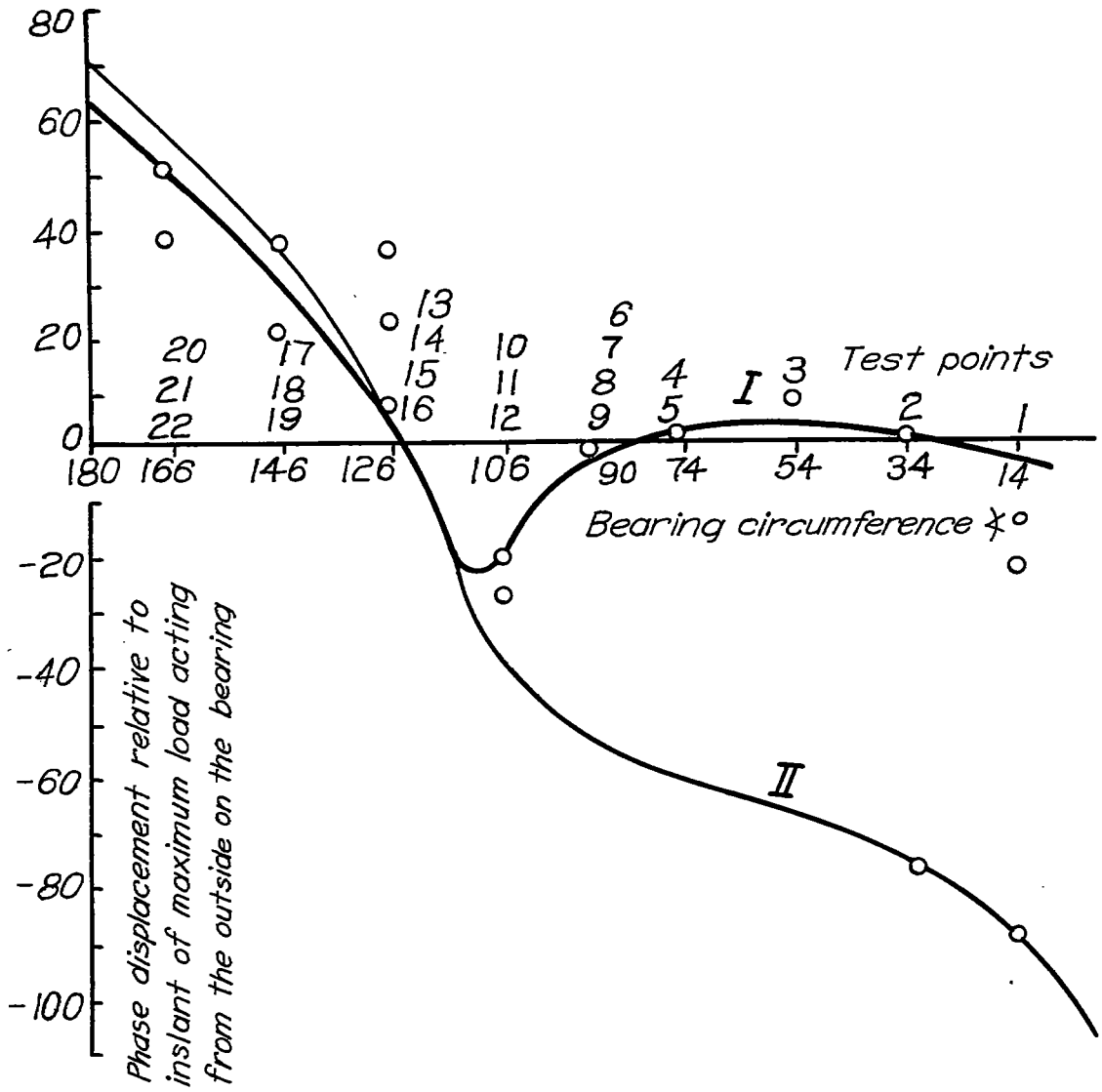

Figure 22 I.- Time-phase displacement of maximum film pressures plotted against the instant of the maximum load acting on the bearing from the outside.

II.- Setting with respect to time of the narrowest lubricating slit in the upper brass as phase displacement plotted against the instant of the maximum load acting on the bearing.

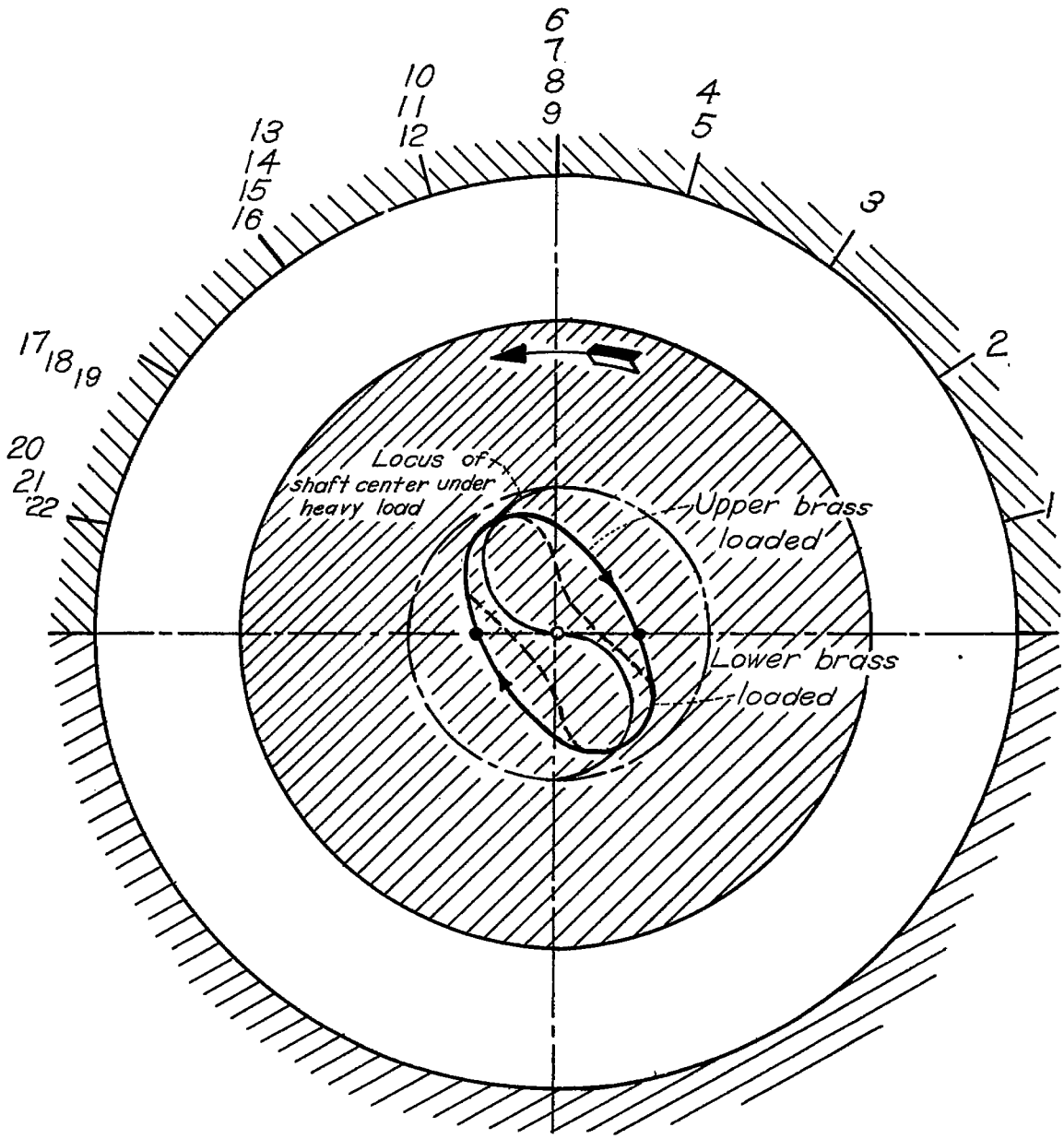

Figure 23.- Orbit of the shaft center.

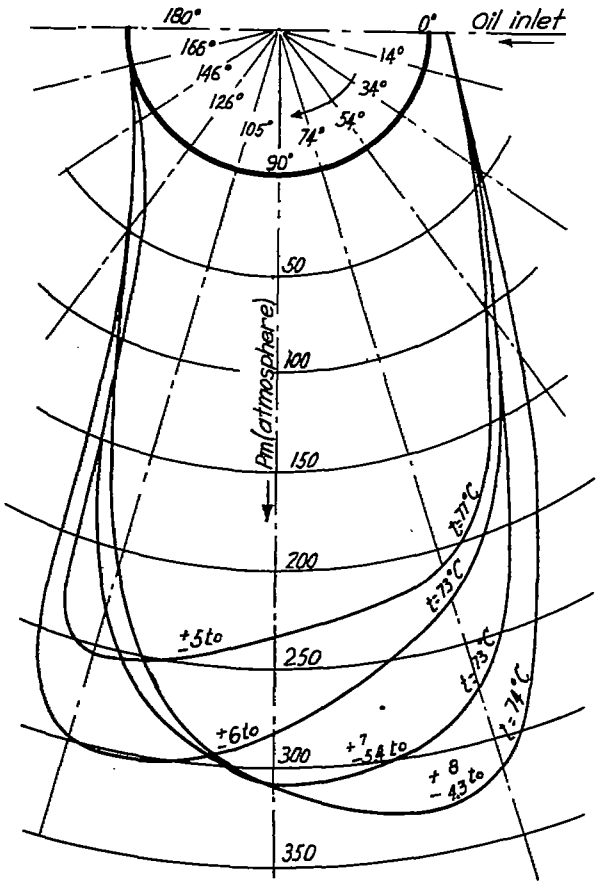

Figure 24.- Bearing cross section with p_m averaged over bearing width for several alternating loads at constant speed = 775 rpm (transition from fluid to semifluid friction) gear ratio 1:1, room temperature 22° C, oil feed pressure 6 atmospheres.

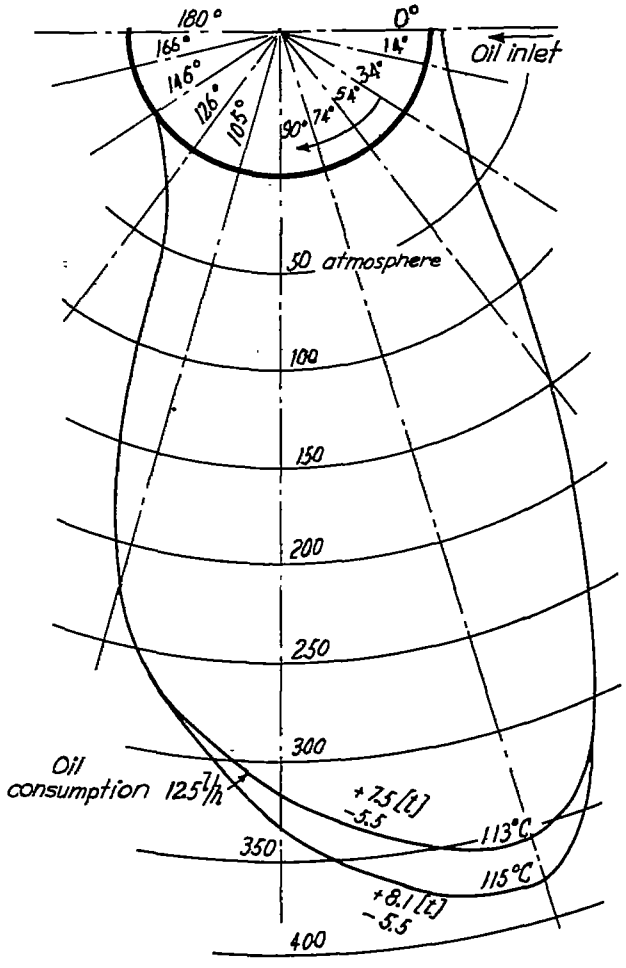

Figure 25.- Bearing cross section with p_m averaged over bearing width for various loads at constant speed. n = 2000 rpm; gear ratio 1:1, room temperature 24° C.